

Title	ニテラ原形質膜の興奮におけるゲーティングの遅れの電気生理学的研究
Author(s)	廣野, 力
Citation	大阪大学, 1983, 博士論文
Version Type	VoR
URL	https://hdl.handle.net/11094/1492
rights	
Note	

Osaka University Knowledge Archive : OUKA

<https://ir.library.osaka-u.ac.jp/>

Osaka University

ELECTROPHYSIOLOGICAL STUDY ON DELAY OF GATING PROCESS

IN EXCITATION OF NITELLA PLASMALEMMA

Chikara Hirono

Department of Biophysical Engineering

Faculty of Engineering Science

Osaka University

March 1983

ELECTROPHYSIOLOGICAL STUDY ON DELAY OF GATING PROCESS

IN EXCITATION OF NITELLA PLASMALEMMA

Chikara Hirono

Department of Biophysical Engineering
Faculty of Engineering Science
Osaka University

March 1983

Preface

Nitella and *Chara* are Characean algae growing in fresh water. Their internodal cells are very large: 0.5 mm in diameter and 2~30 cm in length. Electrical excitation can be produced in those cells by various stimuli, e. g., a current impulse, so that various studies of those cells were made in electrophysiology. As is well known, nerve excitation is explained well by the phenomenological theory proposed by Hodgkin and Huxley. The excitation of plasmalemma in Characean cells, however, has not been analyzed mathematically so well as in the case of nerve excitation, because of experimental difficulties mainly concerning weakness of plasmalemma. In the present study, special specimens were made to observe the excitation in plasmalemma of *Nitella axilliformis*, and some of experimental difficulties were overcome by various devices. Results of analysis proved that the gating process in ionic channels of *Nitella* has a delay which is much longer than in the case of nerve, that is, there is a relatively long time interval between the stimulation and the starting of the gating response.

Major part of this thesis is based upon the contribution of the author to the following two papers.

1. C. Hirono and T. Mitsui: Time course of activation in plasmalemma of *Nitella axilliformis*, in Nerve Membrane - Biochemistry and Function of Channel Proteins, Ed. by G.

Matsumoto and M. Kotani, pp.135-149, University of Tokyo Press, Tokyo, 1981.

2. C. Hirono and T. Mitsui: Slow onset of activation and delay of inactivation in transient current of *Nitella axilliformis*, in press in *Plant & Cell Physiology*, 1983.

A minor part of this thesis has been presented in the book:

T. Mitsui, K. Sugata, C. Hirono and K. Nakanishi; An Introduction to Biophysics - Nerve Excitation and Basic Theory of Thought (in Japanese), Kyoritsu, Tokyo, 1983.

Contents

Summary	1
I. Introduction	
A. Historical Survey of Studies on The Excitable Membranes	4
B. Background of The Present Study	7
II. Experimental Procedures	
A. Preparation of Single Membrane Samples	11
B. Electric Measurements	13
III. Experimental Results	
A. General Properties of The Single Membrane Sample	15
B. Delay of Transient Current	23
C. Time Course of Inactivation in Transient Current	33
D. Excitation Due to Hyperpolarizing Stimulus	36
IV. Model Calculations	
A. Analysis of Delay	39
B. Reconstruction of Action Potential	53
V. Discussion	59
Acknowledgements	68
Reference	69
Appendix	73

Summary

Electrophysiological Studies have been made on the excitation of the plasmalemma of *Nitella axilliformis*. Obtained results have revealed that onset of the activation is very slow and the inactivation starts after a definite delay time in transient current. Results of experimental studies and model calculations in this thesis are itemed as follows:

1. Single membrane samples of internodal cells of *Nitella axilliformis* from which major parts of vacuoles were removed by centrifugation were prepared to analyze the excitation of plasmalemma separately. Experiments were done with these single membrane samples.
2. Resting potential is $-160\sim-100$ mV in the light, and $-140\sim-90$ mV in the dark.
3. Action potential of single membrane samples observed in the light exhibited the smaller peak potential and the shorter duration than that of normal internodal cells which have the tonoplast and the plasmalemma. The action potential in the dark is longer than that in the light. The peak value of the action potential in the dark is as large as that in the light. Under voltage clamp the time course of membrane current in the dark is not quite different from that in the light.
4. Analysis of the experimental data was made by assuming

that membrane current measured by voltage clamp consists of three components: early transient current I_{Cl} , long lasting outward current I_K and leakage current I_L . The transient current occurs only after a initial delay as was observed in *Chara corallina* by Beilby and Coster in 1979.

5. The membrane potential measured at a corner of the sample exhibited almost the same time course as the membrane potential at the center which was changed stepwise, indicating that the delay is not related to the propagation of the potential change.

6. The delay is not sensitive to ionic strength of the external solution, proving that it is not caused by high resistance around the sample.

7. Voltage clamp experiments were made on the delay behavior of I_{Cl} .

8. The time course of inactivation $h(t)$ is investigated from double step experiment.

9. Transient current I_{Cl} during voltage clamp is well reproduced by: $I_{Cl} = \bar{g}_{Cl} m^8 h (V_M - V_{Cl})$, where $m = 1 - \exp(-t/\tau_m)$. The inactivation h has a initial delay δ_h i.e., $h = h_0$ for $t \leq \delta_h$ and $h = h_0 \exp\{(\delta_h - t)/\tau_h\}$ for $t > \delta_h$.

10. On the basis of the above expression of I_{Cl} , the following model is proposed for the gating mechanism of the Cl channel. When membrane potential is changed beyond the threshold, eight m-gates begin to be open. The h-gates start to close after the opening of the m-gates is completed. In

this way, there is a definite delay time for the h-gating.

11. Possibility of excitation due to a hyperpolarizing stimulus was investigated. An excitation was produced by the brief pulse (e.g. 10 ms) of inward current. Hyperpolarizing threshold potential is $-300\sim-450$ mV and decreases with decreasing temperature.

I. Introduction

A. Historical Survey of Studies on The Excitable Membranes

Detailed investigation on the nerve excitation was made possible by using giant axon of squid. The diameter of the giant axon is 1 mm which is 100 times as large as the myelinated nerve of vertebrate (e.g., frog). In the giant axon, a glass microelectrode for potential record and a wire electrode for current supply can be inserted (Hodgkin and Huxley 1939; Marmont 1949).

As for experimental method, voltage clamp technique was developed by Cole et. al. Hodgkin and Huxley (1952 a,b, c) measured membrane current during voltage clamp in external solutions of various Na concentration to analyze the excitation of squid giant axon. They proposed that the nerve excitation is caused by inward sodium current I_{Na} followed by outward potassium current I_K , and that under voltage clamp I_{Na} obeys the m^3h law and I_K obeys the n^4 law. Hodgkin and Huxley established not only phenomenological theory of nerve excitation but also fundamental hypothesis in gating mechanism of ionic channels.

On the other hand, giant algae, *Nitella* and *Chara* have been studied with electrical measurements by many workers for analogue of nerve. Cole and Curtis (1937, 1938) measured the impedance of *Nitella* cells at the resting state and during excitation. Osterhout (1927) measured the potential

difference between the vacuole and the external solution of *Nitella* internodal cells. From the result of measurement of Cl^- efflux and K^+ efflux during the action potential, Gaffey and Mullins (1958) supposed that the excitation of *Chara* involves a transient increase of membrane permeability to Cl^- followed by that to K^+ . Kishimoto (1959) proposed a hypothesis that overshoot of action potential and inward action current are closely related to increased Cl^- efflux during excitation. Walker (1955) inserted glass microelectrodes (3 μm in tip diameter) into the internodal cells of *Nitella* observing them with microscope at high magnification ($\times 500 \sim 1300$). Kishimoto (1959) prepared miniature cells (2 mm long) of *Chara* by centrifugation in which no central vacuoles were observed. Both Walker and Kishimoto reported that the potential in the cytoplasm is very close to the vacuole potential.

In *Chara* and *Nitella*, electrical measurements of excitation are usually carried out via plasmalemma and tonoplast although not only plasmalemma but also tonoplast are excitable. Findlay and Hope (1964) recorded action potentials across the plasmalemma and tonoplast separately. Fig. 1 shows action potentials observed via plasmalemma (A) and via plasmalemma and tonoplast (B). Potential difference via tonoplast changes during excitation so that analysis of excitation of plasmalemma must be done using the data which are obtained from the measurement via plasmalemma separately.

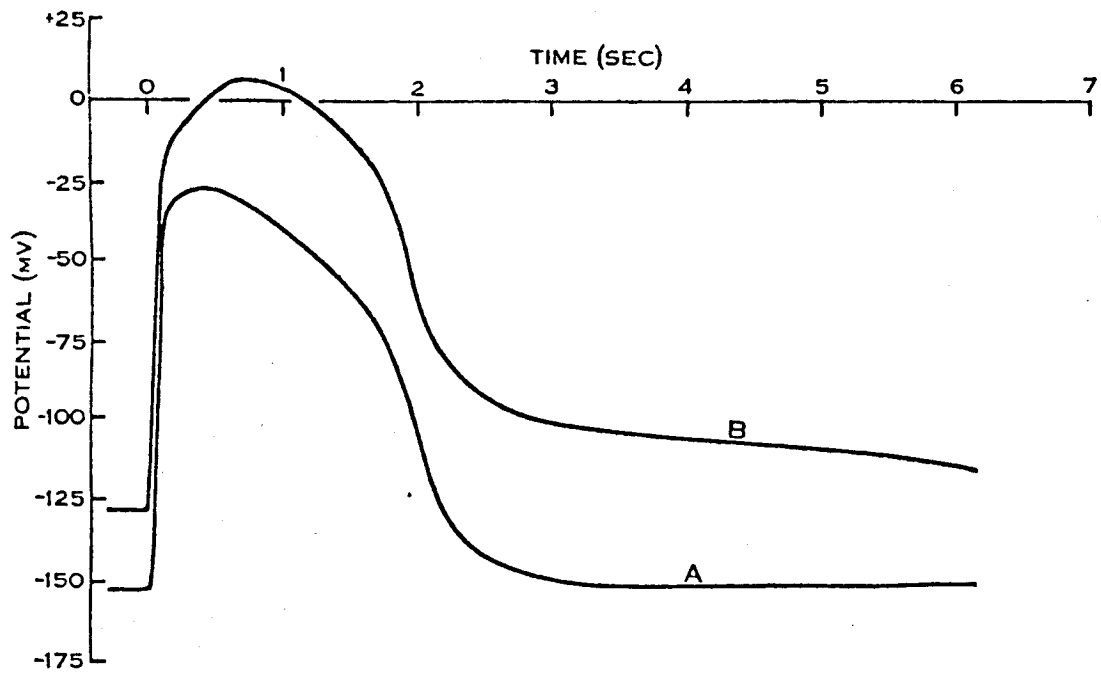


Fig. 1 Action potentials observed via plasmalemma (A) and via plasmalemma and tonoplast (B) in *Chara australis* by Findlay and Hope (1964).

Considering this point, Beilby and Coster (1979 a,b,c) made voltage clamp experiments in detail on *Chara* plasmalemma and proposed its excitation model that the transient current I_{Cl} occurs after a initial delay and then I_{Cl} begins to increase following the m^3h law. They supposed that there is another transient current I_X (presumably I_{Ca}) but not the long lasting outward current I_K .

B. Background of The present Study

In *Nitella* and *Chara*, Cl^- efflux has the same function in excitation as Na^+ influx of nerve as was described in Historical Survey of Studies on The Excitable Membranes. So that transient currents in *Nitella* and *Chara* are presumed to be mainly carried by Chloride ions and the transient current generally called as I_{Cl} . However the transient current I_{Cl} is not expressed by Hodgkin and Huxley's equations because its onset is very slow, compared with I_{Na} in squid giant axons which obeys the m^3h law. Fig. 2 shows the time course of I_{Cl} in *Nitella* (circles and solid line) and the time course of early phase of membrane current ($\div I_{Na}$) in squid giant axon (broken line).

Moreover Hodgkin and Huxley's theory cannot be always applied in nerve excitation because delays in activation and inactivation processes were observed as is described below. Hodgkin and Huxley supposed that inactivation process is independent of activation process and activation and

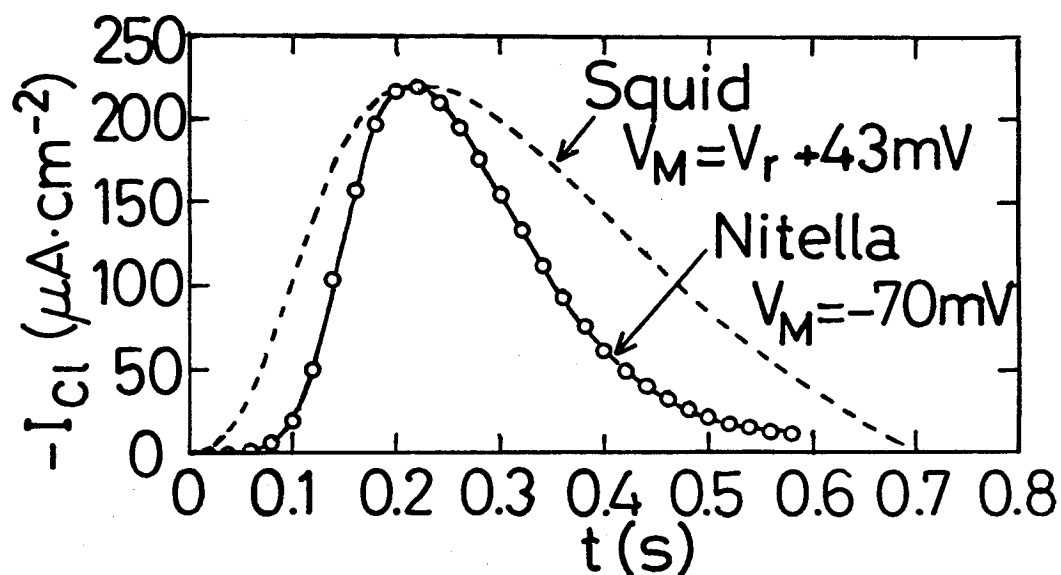


Fig. 2 Early transient current I_{Cl} in *Nitella* (circles and solid line) and early transient phase of membrane current in squid giant axon (broken line). Both of currents in *Nitella* and squid were measured by voltage clamp in which membrane potentials were set to the levels shown in the figure. The scale of the data in squid (Hodgkin and Huxley 1952a) is changed so that the peaks of both currents may fit each other.

inactivation start just after the stepwise change of membrane potential. This assumption is approximately accurate in squid axon if holding potential is set near the resting potential (e.g., -65 mV). Keynes and Rojas (1976), however, found that activation process in giant axon in *Loligo* has a initial delay which increases with decreasing holding potential. Bezanilla and Armstrong (1977) demonstrated a delay of inactivation and proposed that inactivation occurs after channel opening is completed.

As is described in Historical Survey of Studies on The Excitable Membranes, electric measurements in *Nitella* and *Chara* are usually made via two excitable membranes (i.e., plasmalemma and tonoplast). So that the analysis of I_{Cl} is difficult. Beilby and Coster inserted microelectrodes into the cytoplasm of young whorl cells of *Chara corallina*, which have much more cytoplasm between plasmalemma and tonoplast than grown-up internodal cells. They analyzed excitation of plasmalemma by computer simulation and proposed that activation and inactivation of I_{Cl} in *Chara corallina* occur after initial delay and after the delay I_{Cl} follows the m^3h law, that is:

$$I_{Cl} = \bar{g}_{Cl} m^3 h (V_M - V_{Cl})$$

$$\left. \begin{aligned} \frac{dm}{dt} &= 0 \\ \frac{dh}{dt} &= 0 \end{aligned} \right\} \text{ for } t \leq \delta$$

$$\left. \begin{aligned} \frac{dm}{dt} &= \frac{1}{\tau_m} (m_\infty - m) \\ \frac{dh}{dt} &= \frac{1}{\tau_h} (h_\infty - h) \end{aligned} \right\} \text{ for } t > \delta$$

In order to investigate the excitation of *Nitella* plasmalemma, Hirono and Mitsui (1981) prepared single membrane samples from which major vacuoles were removed by centrifugation, following Hayashi (1952), Kamiya and Kuroda (1956). The delay was also observed in these samples. It is important to analyze the delay, because the delay may be closely related to the gating mechanism of Cl channel.

In this thesis the general properties of single membrane samples and the excitation of plasmalemma, especially the delay, are investigated in order to understand the relationships between the delay and the gating process of Cl channel. Model calculations of the transient current I_{Cl} are examined involving Beilby and Coster's model. The best fit between the calculated and observed I_{Cl} is obtained by equations:

$$I_{Cl} = \bar{g}_{Cl} m^8 h (V_M - V_{Cl})$$

$$m = 1 - \exp(-t/\tau_m)$$

$$h = 1 \text{ for } t \leq \delta_h, \quad h = \exp\{(\delta_h - t)/\tau_h\} \text{ for } t > \delta_h.$$

A possible model for gating process in Cl channel is proposed in Discussion.

II. Experimental Procedures

A. Preparation of Single Membrane Samples

The *Nitella axilliformis*, kindly supplied by Dr. K. Kuroda, was cultivated in a glass aquarium of 50 l filled with artificial pond water (0.05 mM KCl, 0.2 mM NaCl, 0.5 mM Ca(NO₃)₂, 0.1 mM MgSO₄, 0.025 mM NaH₂PO₄, 0.025 mM Na₂HPO₄; abbreviated as APW below). It was illuminated with a 15 W fluorescent lamp in a cycles of 12 hours light and 12 hours dark. Its temperature was kept about 25°C. Internodal cells used for the experiments were 2~5 cm long.

Preliminary experiments suggested that the portion of plasmalemma of the internodal cell which is adjacent to the node cells has relatively large electric conductance compared to the other part facing the external medium. This conductive part was isolated by ligation and cut off. The cell with the ligation was cultivated in APW at 25°C with cycles of 12 hours light and 12 hours dark for more than a week. Then the cell was gently centrifuged (200×g, 20~30 min) to bring the cytoplasm to the ligated end and refloat the vacuole from the part. The resulting cytoplasm-rich region was isolated by ligation with thread and used as a sample for experimentation. It was about 1 mm long and 0.3 mm in diameter. Fig. 3 is the photomicrograph of the sample. The cytoplasmic streaming recovered in the sample within 5~30 min after the ligation. Generally vacuoles were not visible in the sample under the microscope just

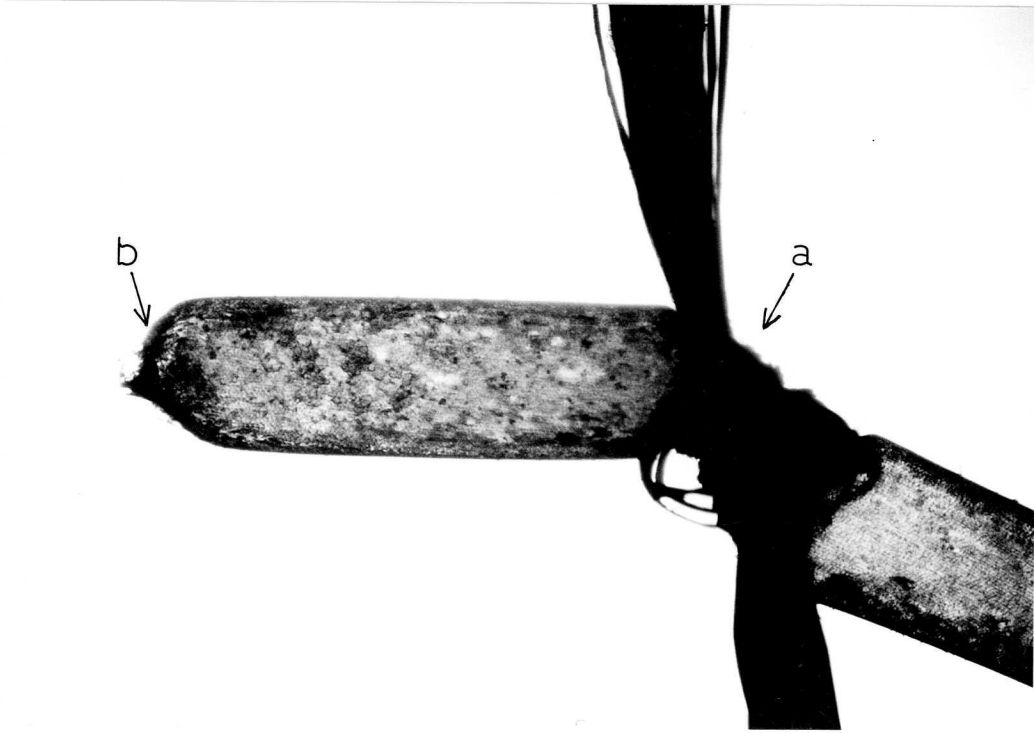


Fig. 3 Photomicrograph of the single membrane sample which consisted of the cytoplasm-rich part of an internodal cell covered with plasmalemma and cell wall. The sample was made by centrifugation and ligation. It was about 1 mm long and 0.3 mm in diameter. A side end of the sample is ligated with thread (a). The thread with which the other end had been ligated was taken off (b). New cell wall had already formed in this region.

after the ligation, but small vacuoles appeared after a day or so. Under the microscope, however, it was easy to insert a microelectrode into the cytoplasm while avoiding the vacuoles. We shall call this a single membrane sample.

B. Electric Measurements

Two glass microelectrodes were inserted into the sample. An agar electrode containing 3M KCl or 0.5 M KCl was placed near the sample for reference to the voltage measurement. Glass microelectrodes were used to supply the stimulus current and to record cytoplasmic potential. Two types of microelectrodes were used, one having a tip diameter of about $1\sqrt{2}$ μm filled with 0.5 M KCl and the other with a smaller diameter filled with 3 M KCl. As reported by Walker (1955) the tip of the electrode was sealed off by a gel-like substance after being in the cytoplasm for $2\sqrt{6}$ hr, causing an apparent rise of the resting potential. The 0.5 M KCl electrodes were more stable against this obstruction than the 3 M KCl electrodes and were used for most of the measurements.

The circuit for clamping voltage and measurement of the membrane current was a modification of the one used by Kishimoto (1968). Details about the circuit are described in Appendix. Membrane potential and current were sampled at $1\sqrt{10}$ ms intervals, converted to digital data and recorded on the magnetic tape. (see Appendix)

Temperature were measured with a copper-constantan

thermocouple or a thermistor (Shibaura Electronics, LSB type) and recorded with a pen recorder (Matsushita Com. In. Co., VP654B). The temperature of the vessel in which the sample was placed was controlled by circulating temperature-controlled water in contact with the outside of a polyethylene tube which guided the external medium from a flask into the vessel. The temperature of the circulating water was controlled by a thermo-electric device (Yamato Kagaku Co., Coolnics).

III. Experimental Results

A. General Properties of The Single Membrane Sample

In this chapter description is made about the resting potential and the action potential of the single membrane sample measured in the external solution APW (pH: 6.0).

Resting potential

The resting potential of single membrane samples is $-160\sim-100$ mV in the light. When the light is turn off, the resting potential increases to $-140\sim-90$ mV. Fig. 4 shows an example of potential change induced by turning the light on and off. The resting potential in the light is -150 mV. When the light is turn off, the membrane potential changes with the time constant of 20 min to -110 mV. After leaving the sample in the dark for 65 min, the light was turn on that caused hyperpolarizing after the dead time of 30 min. Usually membrane potential recovered with the time constant of $20\sim40$ min. The sample of which the resting potential in the light is smaller than about -140 mV exhibits large potential change (i. e., 40 mV) at turning off and turning on the light. But the sample of which the resting potential in the light is larger than about -120 mV does not exhibit the change after turning off and turning on the light.

The distribution of the resting potential of many samples in the light and in the dark is shown in Fig. 5.

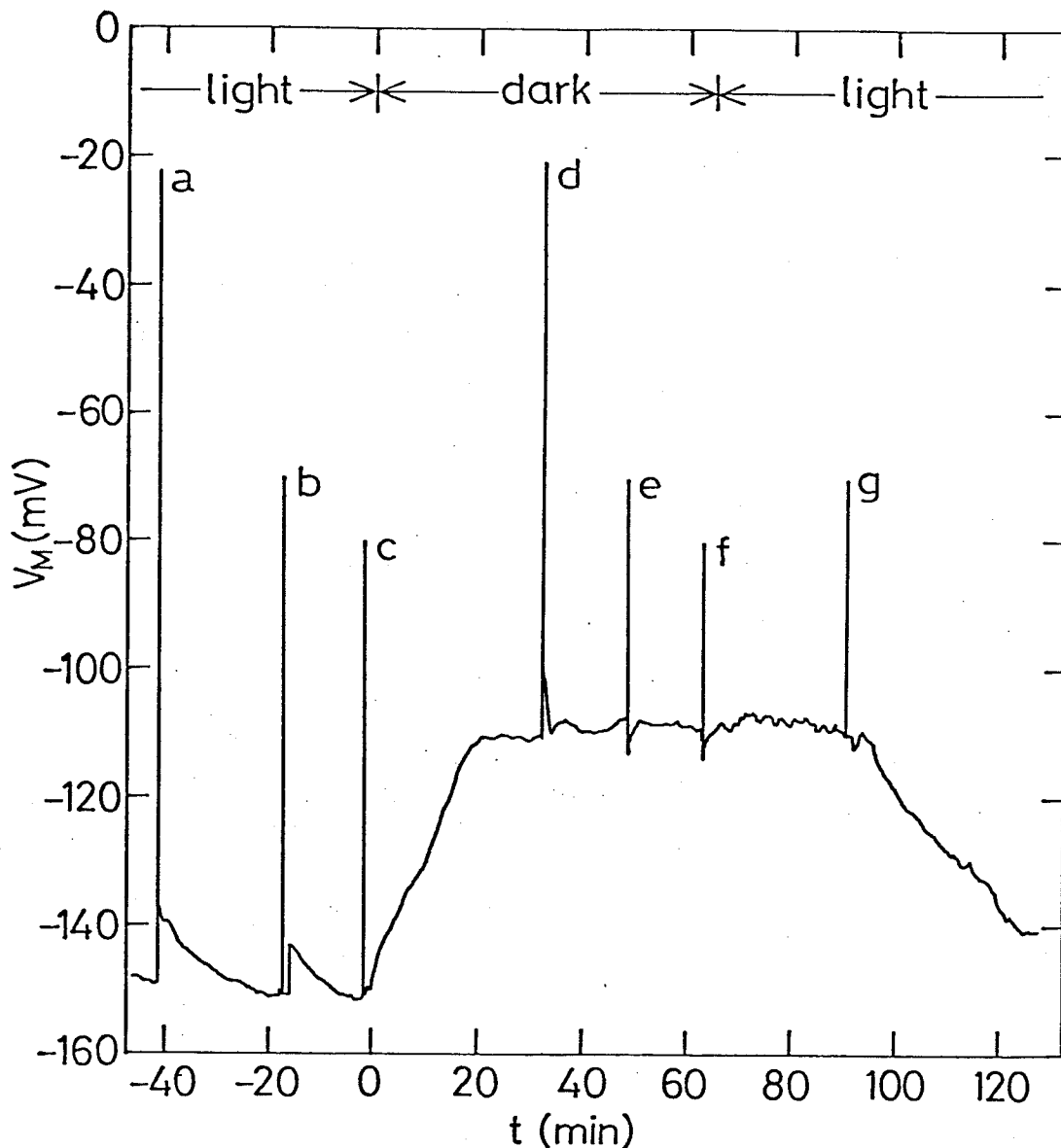


Fig. 4 The level change of resting potential induced by turning off and turning on the light. The pulses a and d in the figure are action potentials caused by current stimulation; other pulses b, c, e, f and g are potential changes during voltage clamp of 10s. The resting potential in the light was about -150mV. When the light was turned off at $t=0$ the resting potential increased monotonously to about -110mV and then became stable at -110mV. When the light was turned on at $t=65$ min the resting potential began to decrease after the time interval of about 30min. Sample:820907-II.

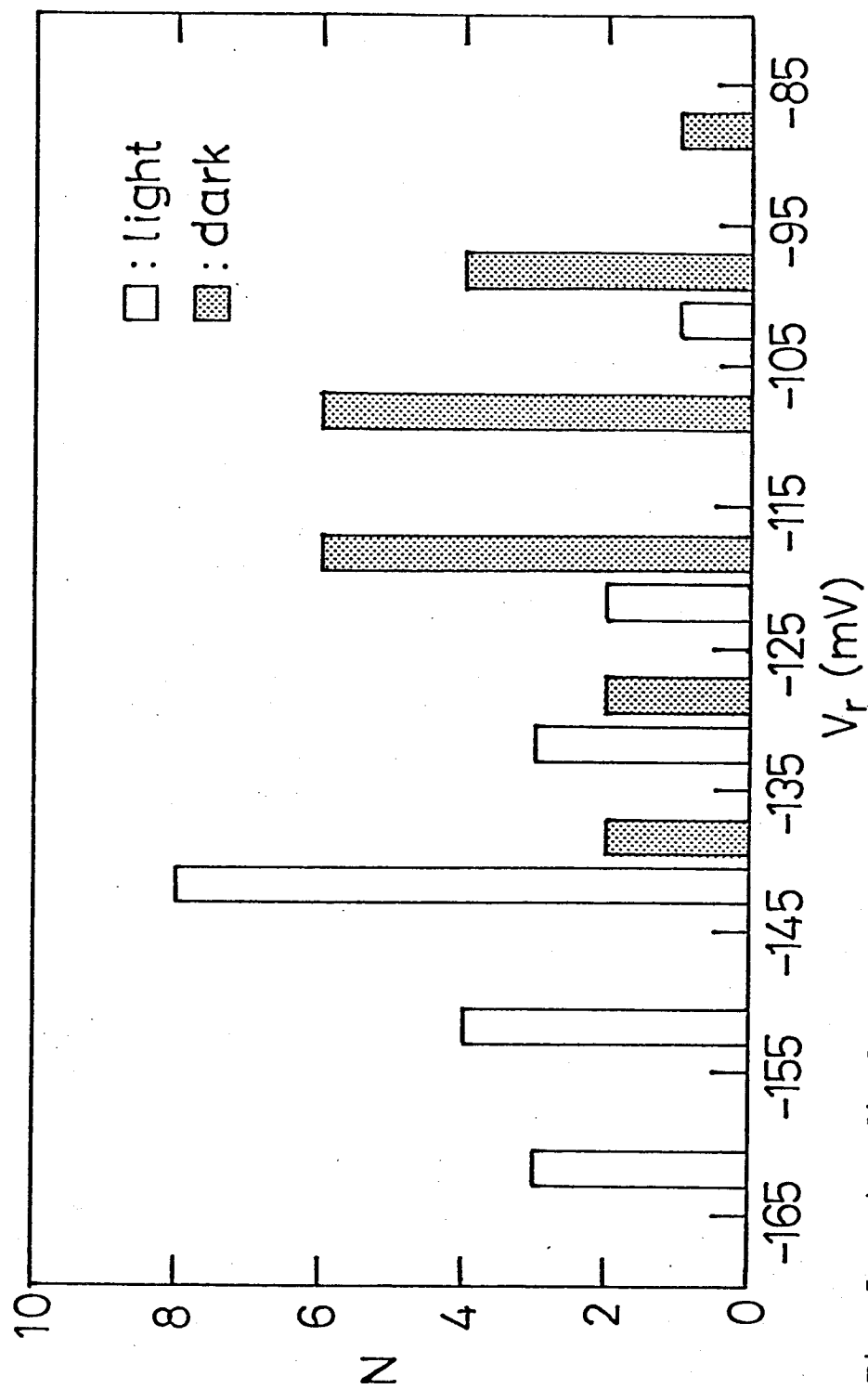


Fig. 5 Histodiagram of the resting potential of single membrane samples in the light (\square) and in the dark (▨). The number of samples of which the resting potential is included in the interval of potential is accumulated in every 10 mV intervals. The samples were counted in which both of the resting levels in the light and in the dark were measured.

Action potential

The action potential took place when the stimulation with pulsed current exceeded a threshold (e.g., $5 \mu\text{A cm}^{-2}$, 50 ms). An example of the action potential in the light is shown in Fig. 6A, in comparison with that of the normal internodal cell, i.e., the one observed via plasmalemma and tonoplast (Fig. 6B). For this comparison the internodal cell was ligated to make its size about the same as the single membrane sample. The action potential in Fig. 6A has a shorter duration and smaller peak height than that in Fig. 6B.

The excitation of the sample was of the all-or-none type as shown in Fig. 7. When the stimulating current was smaller than $5 \mu\text{A cm}^{-2}$, only an RC response was observed. But increasing the amplitude of the current to $5 \mu\text{A cm}^{-2}$ resulted in an action potential. The peak of the action potential was constant in response to stimulation of various amplitudes over the threshold (e.g., 5, 6.1, 9.2 and $16.7 \mu\text{A cm}^{-2}$).

The peak value of action potential in many samples is -21 ± 6 mV (\pm S.D.) in the light which is almost the same as those in the dark as shown in Fig. 8.

The half-maximum width of action potential is about one second in the light at 24°C which is smaller than that of action potential in the dark. Fig. 9 shows an action potentials in the light (a) and in the dark (b).

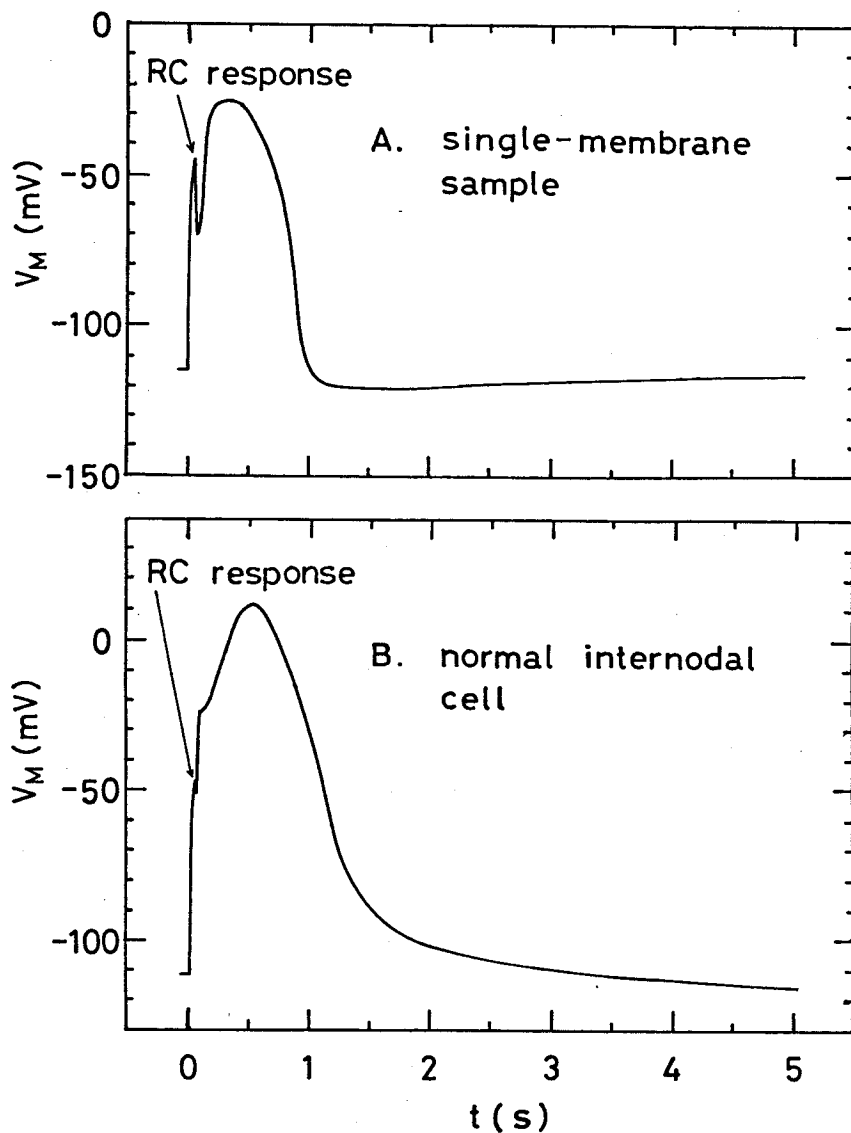


Fig. 6 Action potentials of a single membrane sample (A) and a normal internodal cell (B). The samples were almost the same size (1.1 mm long and 1.2 mm² in surface area). Stimuli were pulsed current of 5 $\mu\text{A}\cdot\text{cm}^{-2}$ (A) and 1.8 $\mu\text{A}\cdot\text{cm}^{-2}$ (B), 50 ms in duration. Temperatures were 25.7°C (A) and 25.5°C (B). The external medium was artificial pond water (0.05 mM KCl, 0.2 mM NaCl, 0.5 mM Ca(NO₃)₂, 0.1 mM MgSO₄, 0.025 mM NaH₂PO₄ and Na₂HPO₄). Sample (A): 790918; normal internodal cell (B): 790917.

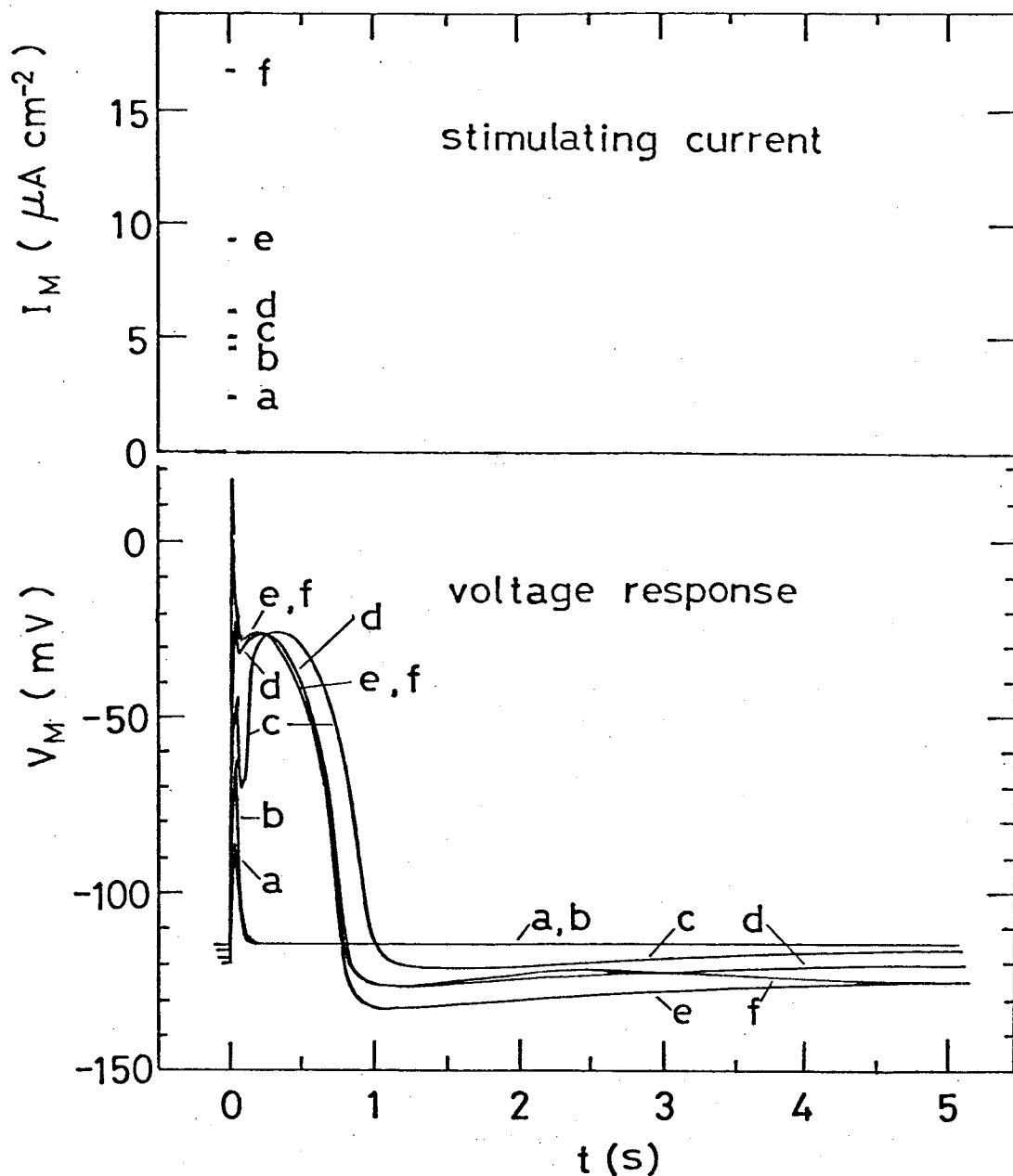


Fig. 7 All-or-none response of the single-membrane sample. Upper traces are stimulating currents and lower traces are the voltage response. Initial peaks of potentials are an RC response of plasmalemma. Action potential did not result from stimulation of less than $5 \mu\text{A}\cdot\text{cm}^{-2}$, 50 ms (a,b), but did occur at $5 \mu\text{A}\cdot\text{cm}^{-2}$ (c). When the current amplitude was increased (d,e,f), the action potentials had approximately the same time course except for the parts of undershoot. External medium was APW. Sample: 790918.

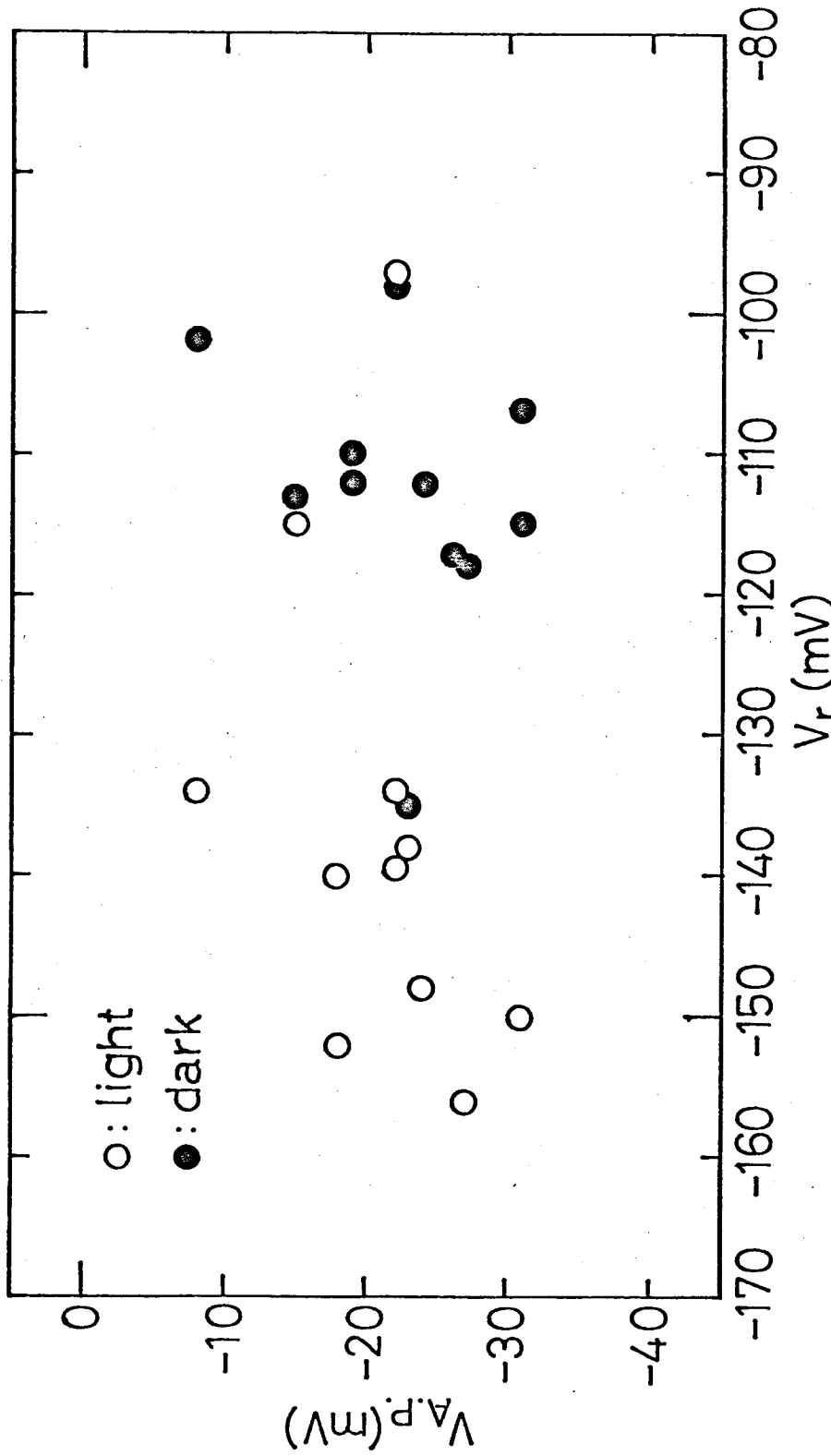


Fig. 8 Distribution of the peak of action potential $V_{A.P.}$ (ordinate) vs. the resting potential (V_r) in single membrane samples. The sample was selected in which both of measurements in the light and in the dark were made. There is practically no difference between $V_{A.P.}$ in the light and one in the dark, and no correlation between the resting potential V_r and $V_{A.P.}$.

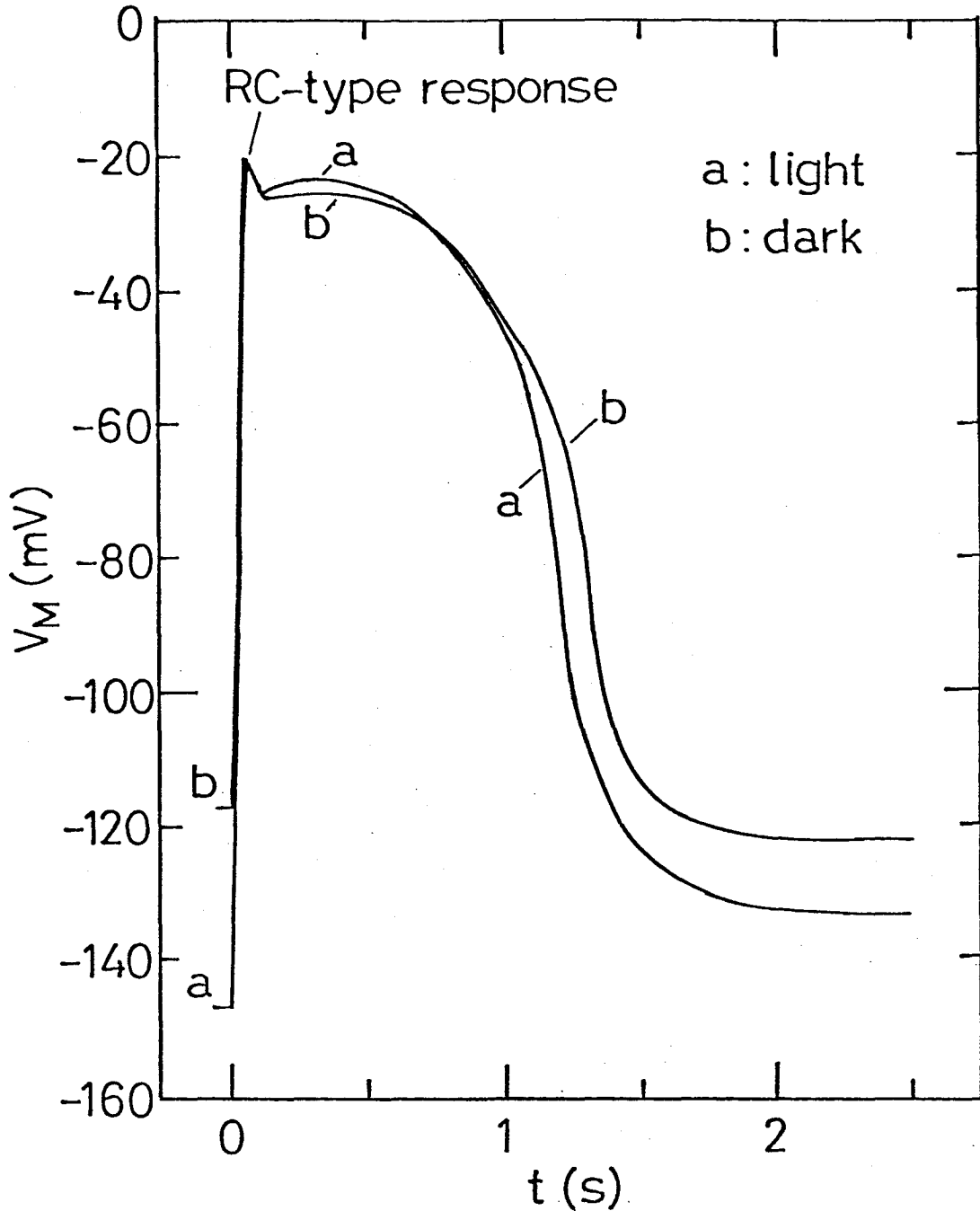


Fig. 9 Examples of action potentials in the light (a) and in the dark (b). The action potentials a and b exhibited practically the same peak-values, although the resting levels are different from each other. Duration of action potential in the dark is slightly larger than that in the light. The first peak in each trace is RC-type response by current stimulation. Temperature was 24°C. Sample: 820907-I

B. Delay of Transient Current

In this chapter the results are reported of investigation on the property of transient current, especially a delay in the current response, observed by voltage clamp.

Membrane current during voltage clamp

In the voltage clamp experiment, the stepwise change of membrane potential over threshold (about -95 mV) across the plasmalemma of the single membrane sample resulted in the current response of early transient phase, followed by slowly increasing outward phase. It is generally accepted that the membrane current I_M consists of two components except for minor leakage current I_L . One is the early transient current and the other is slowly increasing outward current. Major part of the former is carried by Cl^- ions (and presumably by K^+ ions as noticed in Discussion) and latter by K^+ ions. Following the tradition, the early transient current and the latter are denoted by I_{Cl} and I_K , the corresponding channels by Cl channel and K channel, the corresponding ion conductance by g_{Cl} and g_K and the corresponding reversal potential by V_{Cl} and V_K , respectively. The contributions of I_{Cl} , I_K and I_L to the membrane current I_M were very different in different samples. The sample was chosen for which I_K and I_L were very small in a limited domain of time and membrane potential, so that the properties of I_{Cl} could be studied separately. Fig.10 shows the membrane current I_M at various V_M . In Fig.10, the inward transient

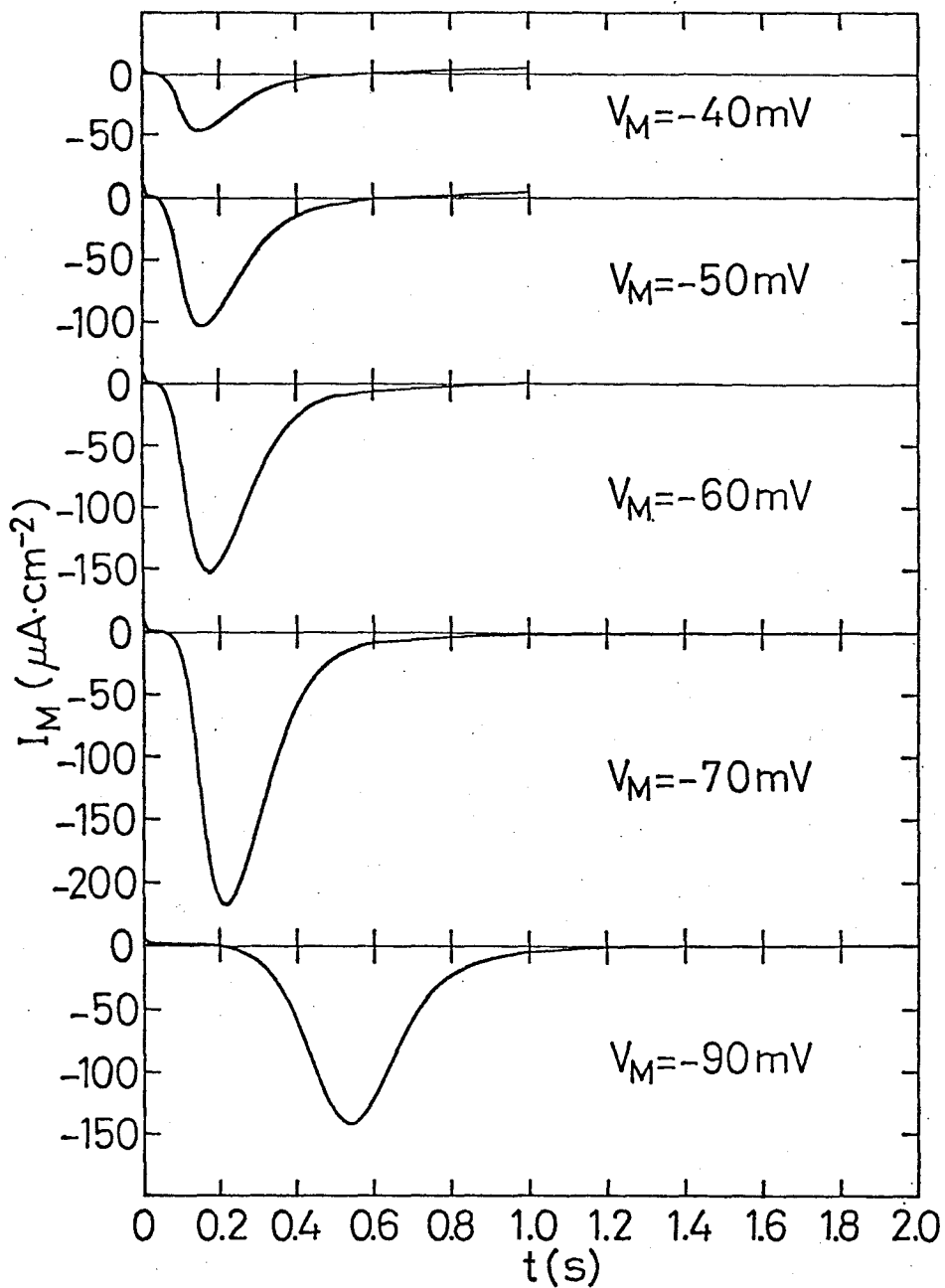


Fig. 10 Membrane current I_M through plasmalemma of *Nitella axilliformis* measured by voltage clamp technique. Membrane potential was changed stepwise at $t=0$ from the resting level of -140 mV to the level of V_M indicated in each figure. Temperature was 23.7°C . Sample: 810515.

current I_{Cl} is pronounced compared to the slowly increasing outward current I_K , which becomes appreciable only for $V_M \geq -50$ mV. The peak value of $|I_{Cl}|$ becomes maximum at -70 mV in Fig.10. It decreases with increasing V_M and extrapolation of this data suggests that the peak value becomes zero at V_M of -31.5 mV. This reversal potential will be denoted as V_{Cl} below.

Apparent delay in activation of I_{Cl}

Fig. 10 demonstrates that there is a time interval between the stepwise change of V_M at $t=0$ and the moment when change of I_M becomes appreciable i. e., there is a delay in the occurrence of the inward transient current I_{Cl} . The delay is large at -90 mV and decreases with increasing V_M . The time of break point of activation, i. e., the apparent delay time δ' decreases with increasing temperature as in *Chara* (Beilby and Coster, 1979 a, b, c). Fig. 11 shows temperature dependence of δ' at various V_M . Data points in Fig. 11 is only three in each V_M , but data of the other samples exhibit the similar property.

Some checks about the factor of delay

During the measurements a doubt arose whether the delay of the membrane current is related to the low electric conductance of the external solution and / or the light illumination and / or propagation of the membrane potential change. The low electric conductance might result in a large

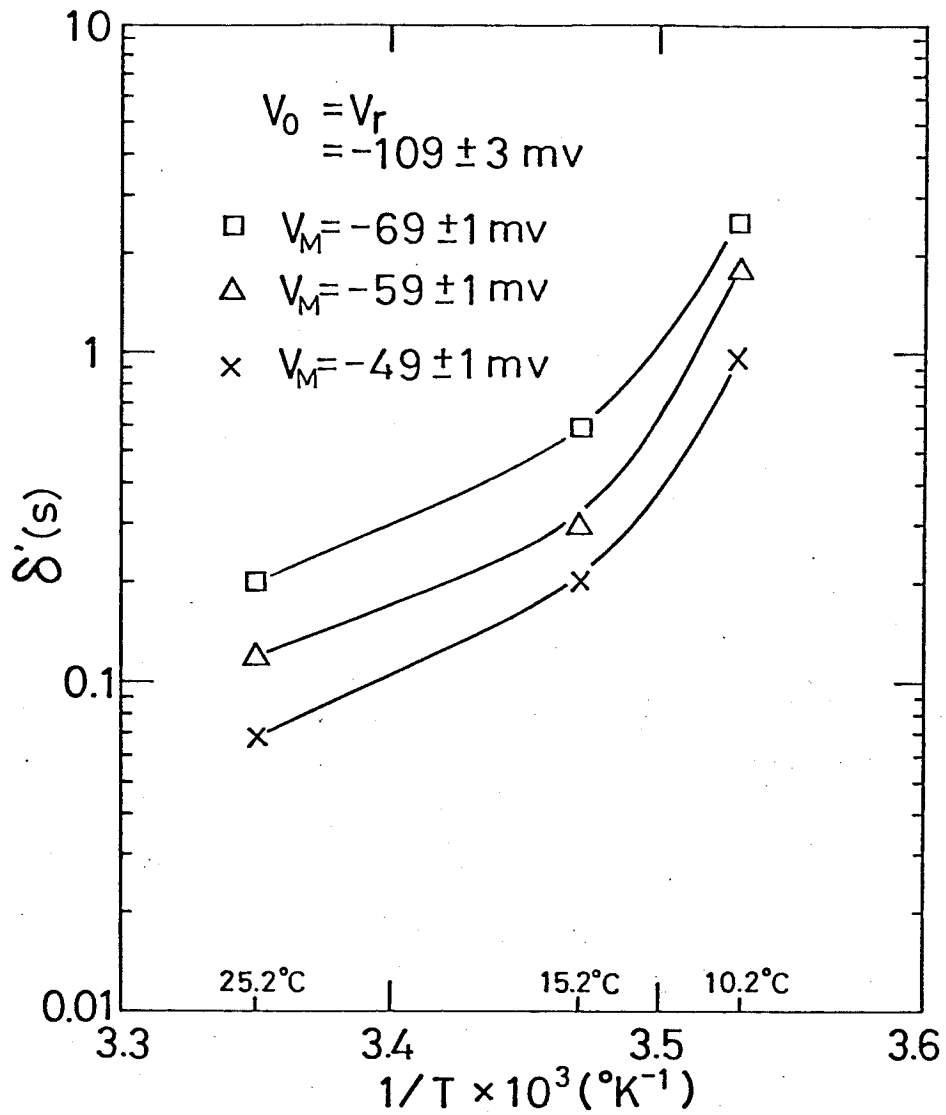


Fig. 11 Temperature dependence of an apparent delay time δ' which is defined as the time of break point in the rising phase of I_{Cl} . The clamp potential is different in each symbol as shown in the figure. Sample: 790707.

time constant in charging the membrane capacitance and in an error in clamped membrane potential by large series resistance. The electrogenic pump enhanced by light might make the time course of the membrane current in the light different from that in the dark. The propagation could cause an apparent delay since the current source in the sample was point-like and thus space clamp of the membrane potential was not assured strictly.

(i) *Effect of high resistance of external solution on the delay*

In order to examine the effect of the low conductance of the external solution, the membrane current was measured under voltage clamp first in APW and then in high ionic-strength solution and again in APW. The high ionic-strength solutions were made by adding 10 mM LiCl, or 5 mM Li₂SO₄ or 5 mM Na₂SO₄ to APW. The current measurements were done longer than 10 min after changing the external solution. Fig. 12 shows the membrane current after stepwise change of the membrane potential at t=0 from the resting potential V_r (about -120 mV) to -80 mV. The curve a is the result of the first measurement in APW. The curve b is the result in the high ionic-strength solution of APW + 10 mM LiCl. The curve c is the result in APW again. As is usually observed, there was a steady change in the current curve after immersing the specimen in the high ionic-strength solution. But if we normalize the curves by putting the maximum of the inward current equal to one, the initial

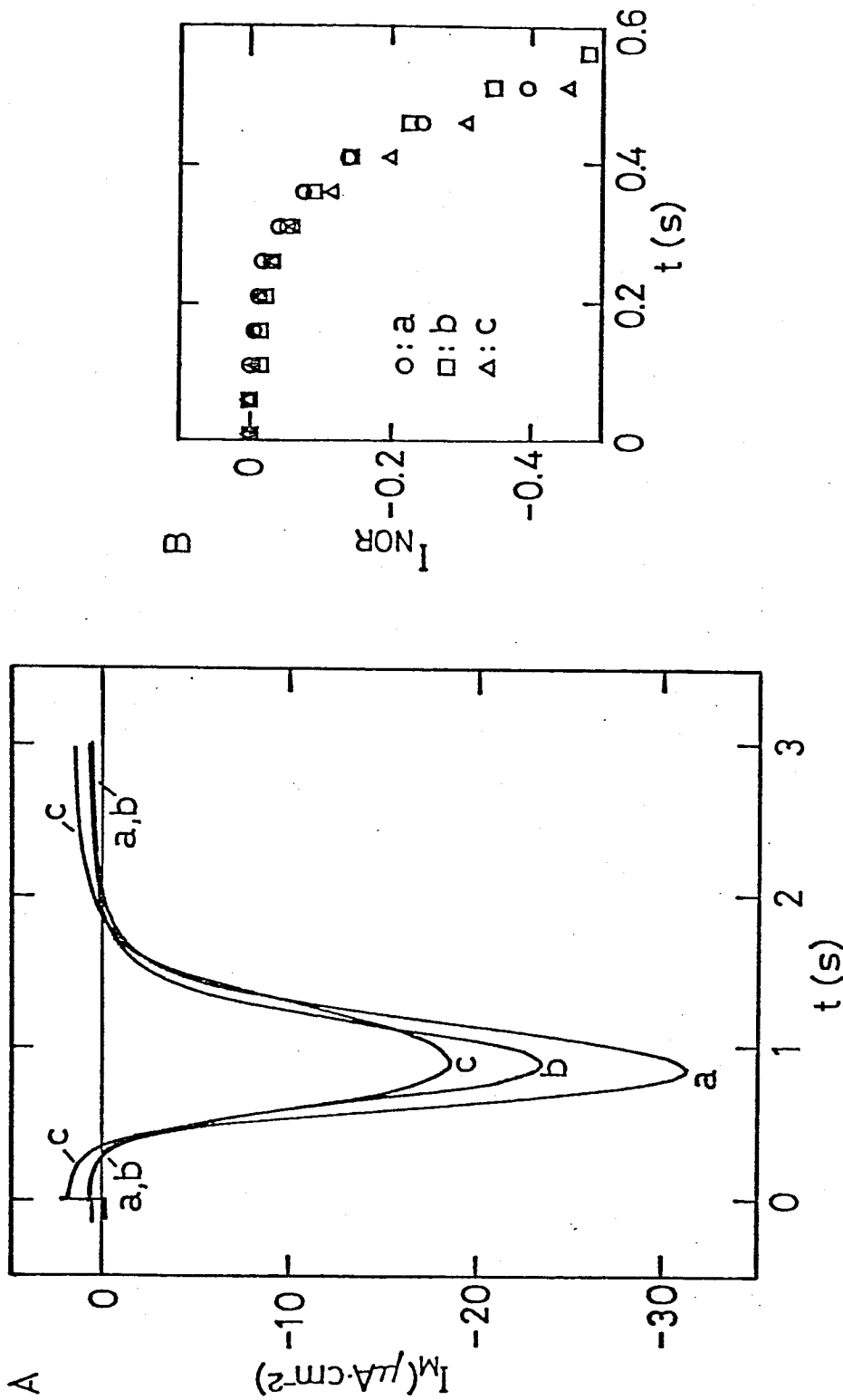


Fig. 12 Membrane currents I_M through plasmalemma when the membrane potential was changed stepwise at $t=0$ from the resting level of the specimen used (-120 mV) to -80 mV. (A) Measured I_M . Temperature was 22.3°C. a: in APW. b: in high ionic-strength solution (APW+10 mM LiCl). c: in APW again. (B) Normalized transient current: $I_{\text{NOR}} = [I_M(t) - I_M(0)] / I_p$ where I_p is the peak value of the transient current, i. e., $|I_M(t) - I_M(0)|_{\text{max}}$. Sample: 800909.

parts of the curves become almost the same, as shown in Fig. 12, indicating that the delay behaviour is not sensitive to the ionic strength. Similar experiments were repeated nine times using the various high ionic-strength solutions described above. In these cases we defined an apparent delay time as the time where the tangent of the current curve $I(t)$ at the maximum negative slope intersects the straight line which passes the initial value of the current $I(0)$ and is parallel to the abscissa. The apparent delay time changed only within the range of -30 % to 8 % against 5.2 to 7.7 times increase of the ionic strength in the external solution. These results prove that the low electric conductivity of the external solution is not an origin of the delay in current response.

(ii) *Effect of electrogenic pump enhanced by light on the delay*

Many workers reported that plasmalemma of Characean cells have electrogenic ion pump which is sensitive to light, pH of external solution, temperature and metabolic inhibitor and correlated to ATP concentration in cytoplasm (Kitasato 1961; Saito and Senda 1974; Richards and Hope 1974; Shimmen and Tazawa 1977; Kishimoto, Kami-ike and Takeuchi 1980, 1981).

Voltage clamp experiments in this thesis were usually carried out in the light. There is a possibility that the delay behaviour is caused by the light effect, e. g., by the contribution of electrogenic pump which is depressed

in the dark as shown in Fig. 4. So that it was examined whether the delay behaviour in the dark is not different from that in the light. Fig. 13 shows membrane currents I_M measured first in the light (a), the second in the dark (b) and the third in the light (c). The time course of I_M in the light (a) is not quite different from I_M in the dark (b). This fact indicates that the light does not affect to the delay. Sometimes the amplitude of the current measured in the dark is much smaller than that in the light. Discussion will be done about this point in Discussion.

(iii) *Propagation of membrane potential change*

In order to examine whether the delay is related with propagation of the membrane potential change, we measured the membrane potentials simultaneously at the center and the corner of the single membrane sample which was cylindrical in shape, with the diameter of 0.34 mm and the length of 1.7 mm, which is longer than those used in other experiments. Results are shown in Fig. 14. The curve V_a is the clamped membrane potential at the center of the specimen, and V_b is the membrane potential at the corner. There is no delay in V_b against V_a , indicating that the delay in the current response is not related with the propagation of the membrane potential change. The potential V_b is smaller than V_a by 2~3 mV presumably

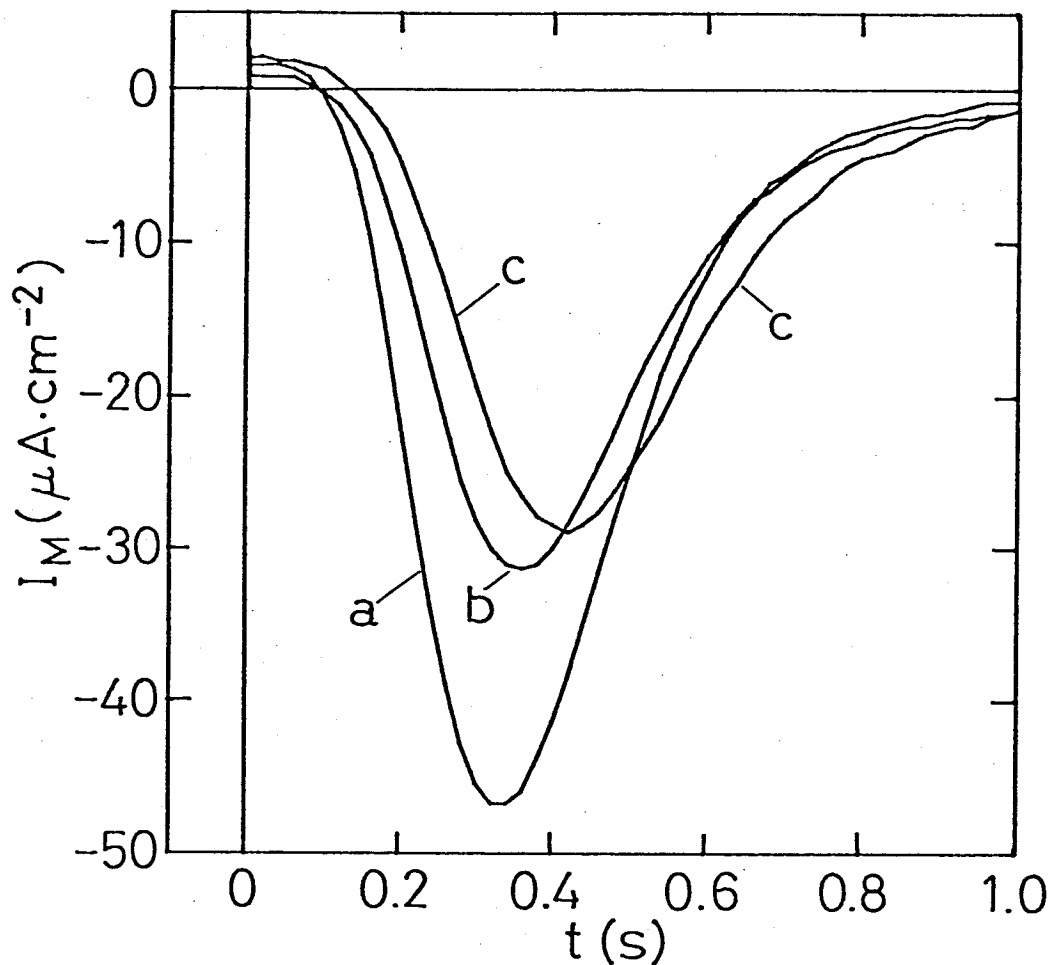


Fig. 13 Membrane currents I_M measured first in the light (a) and then in the dark (b) and again in the light (c). Each measurement was made by voltage clamp from resting potential when the resting level became steady, (a: -141mV b: -115mV c: -141mV) to -60mV. Temperature was 23.7°C. Sample: 820910.

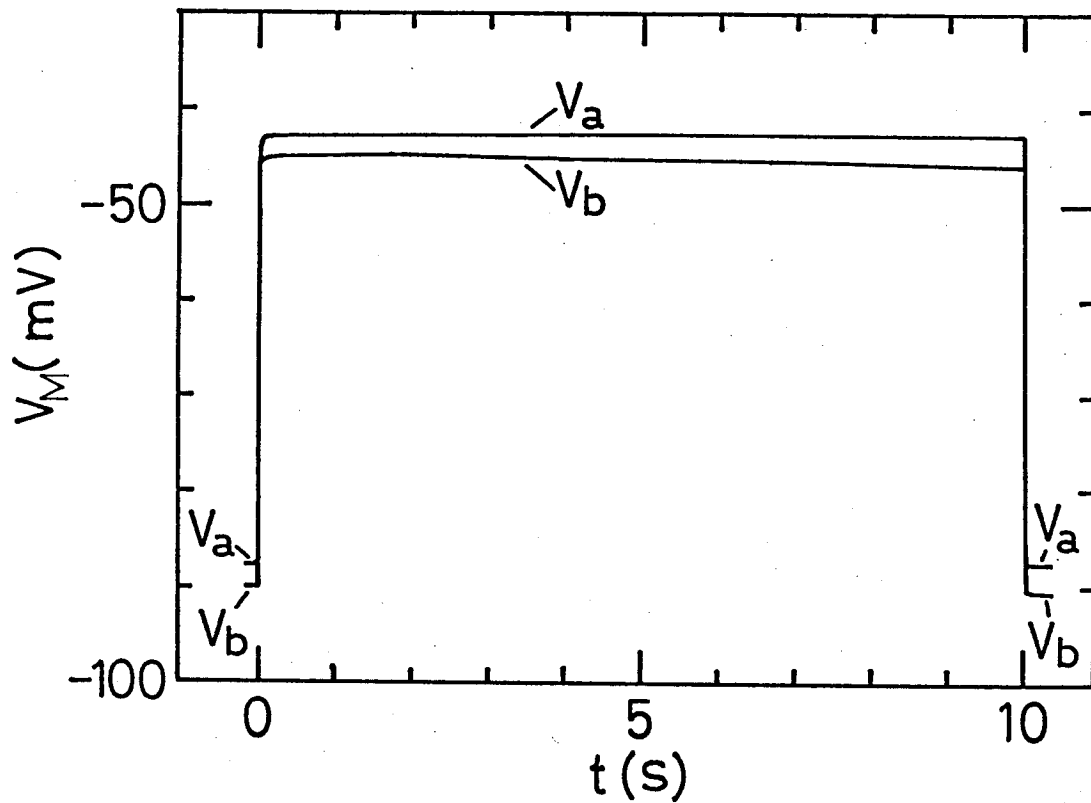


Fig. 14 Simultaneous record of membrane potentials at different positions in a single membrane sample which is cylindrical with the length of 1.7 mm and the diameter of 0.34 mm. V_a : clamped membrane potential at the center of the sample. V_b : membrane potential measured at the corner. The external solution was APW. Temperature was 23°C. Sample:791215.

because of a difference in tip potentials of the micro-electrodes. Resting potential of this sample was larger than usual, presumably due to damage of the membrane by the inserted three electrodes: one for current supply and two for potential recording.

C. Time Course of Inactivation in Transient Current

Following Hodgkin and Huxley (1952b), time course of inactivation $h(t)$ was tried to observe by changing the clamp potential in two steps. That is: Membrane potential was changed at $t=0$ from resting potential V_r to V_1 (-70 mV) and then at various time ($t_1 \sim t_8$) from V_1 to V_2 (0 mV) as shown in Fig. 15a. The peak value of transient current I_{Cl} corresponding to each second step will be approximately proportional to $h(t)$ at $V_M=V_1$ because $\tau_m(V_2)$ is much smaller than $\tau_h(V_2)$. The current data in which membrane potential was changed to the second step at t_1 , t_2 and t_3 exhibited the same peak values, suggesting that there is a delay in inactivation process. Fig. 16 shows the time course of inactivation $h(V_1, t)$, where the circles are the normalized peak values of outward transient current I_{Cl} at V_2 in Fig. 15b.

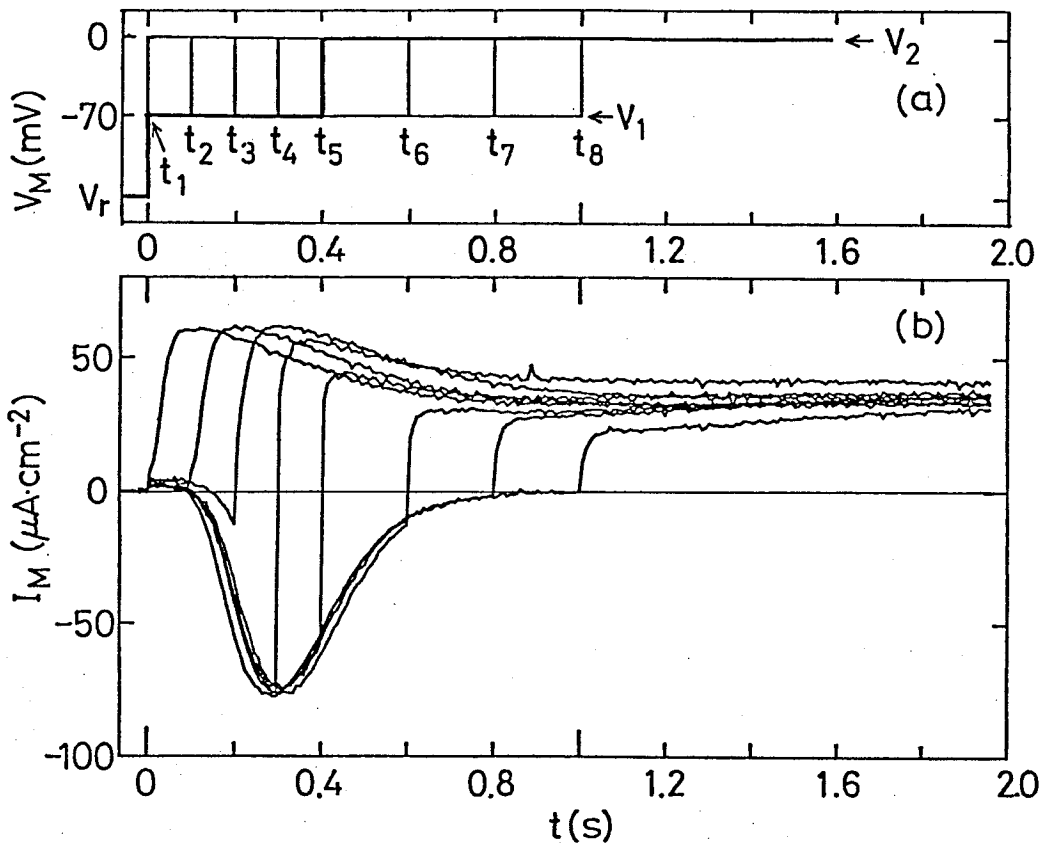


Fig. 15 Experimental demonstration of delay in inactivation by voltage clamp. (a): Two step changes of membrane potential V_M . The membrane potential is changed from V_r to V_1 at $t=0$ and then to V_2 at various times (i. e., $t=t_1, t_2, \dots$ or t_8). (b): Observed membrane currents for eight measurements when the membrane potential was changed as shown in (a). The peaks of outward transient currents corresponding to the second stepwise changes at t_1, t_2 and t_3 are almost the same values, suggesting the existence of the delay in inactivation. Sample: 820929.

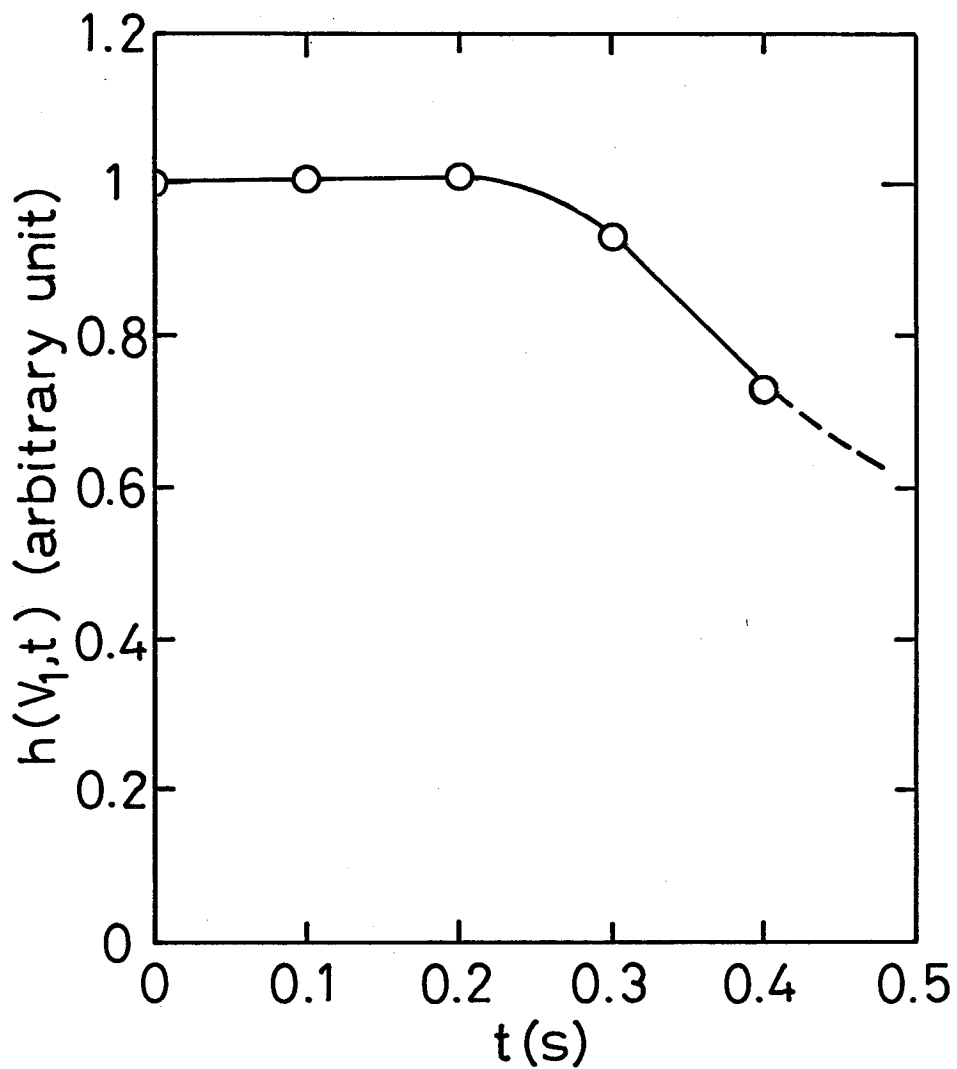


Fig. 16 Time course of inactivation $h(V_1, t)$, where V_1 is the voltage of first step in Fig. 15a (i. e., -70 mV). Data point (circles) are the peak values of outward transient current in Fig. 15b, where abscissa is the time of the V_M change from V_1 to V_2 .

D. Excitation due to Hyperpolarizing Stimulus

The excitation of the giant axon of squid can be taken place not only depolarizing stimulus but also by hyperpolarizing stimulus (Hodgkin and Huxley 1952c, FitzHugh 1976). This phenomenon was also observed in two membrane system of plasmalemma and tonoplast of *Chara* (Ohkawa and Kishimoto 1975). In the present study, it is examined whether the single membrane sample of *Nitella axilliformis* can be made exhibited the excitation by brief stimulus of inward current. Fig. 17 shows the response of the single membrane sample to the brief inward current (50 ms). When the current amplitude is smaller than the threshold RC response of negative direction and subthreshold response of positive direction are observed. But making the amplitude larger than the threshold, the excitation occurs. The excitation is all-or-none type and its shape is similar to that induced by outward current stimulus.

The hyperpolarizing threshold potential was measured which is defined as the negative peak potential of RC response to brief inward current of minimum amplitude to induce the excitation. As shown in Fig. 18 temperature dependence of the hyperpolarizing threshold potential has positive slope against temperature that is different from the case of squid giant axon (FitzHugh 1976; Nakanishi 1980).

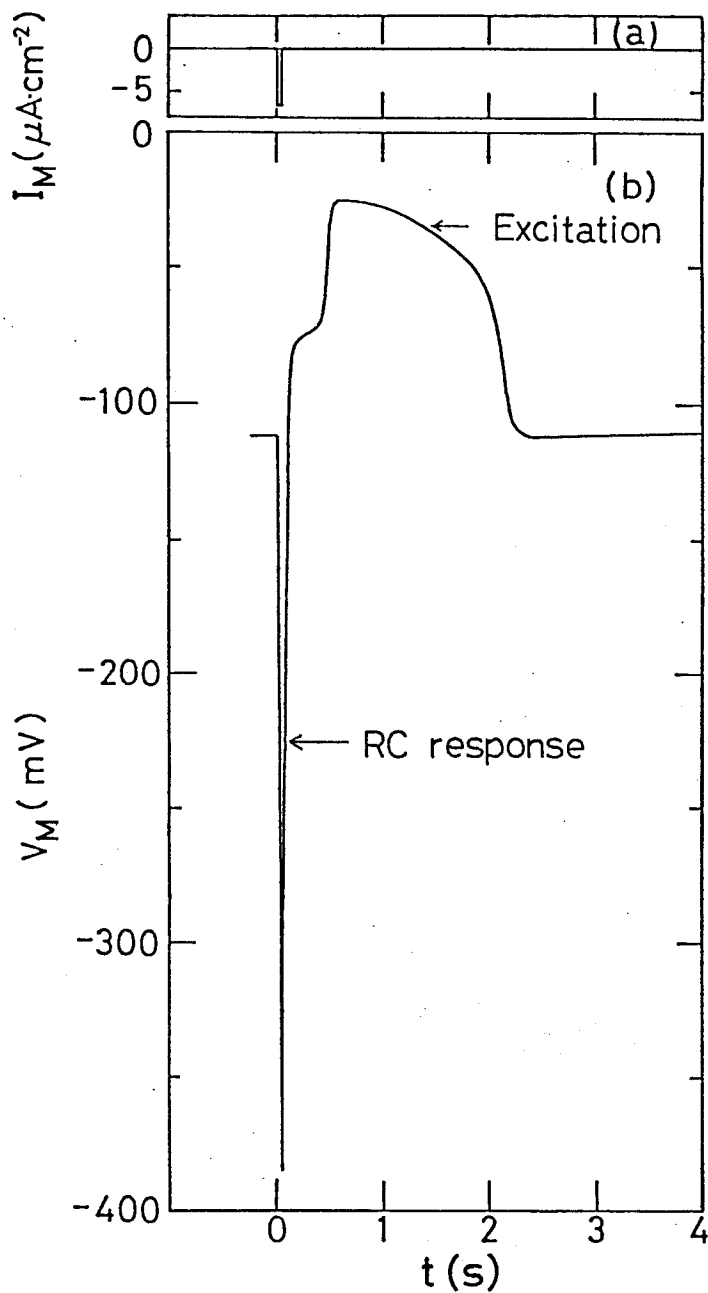


Fig. 17 Action potential induced by hyperpolarizing stimulus. (a): Stimulating current of 50 ms in duration. (b) Voltage response of the specimen. Temperature was 22.5 °C. Sample: 800214.

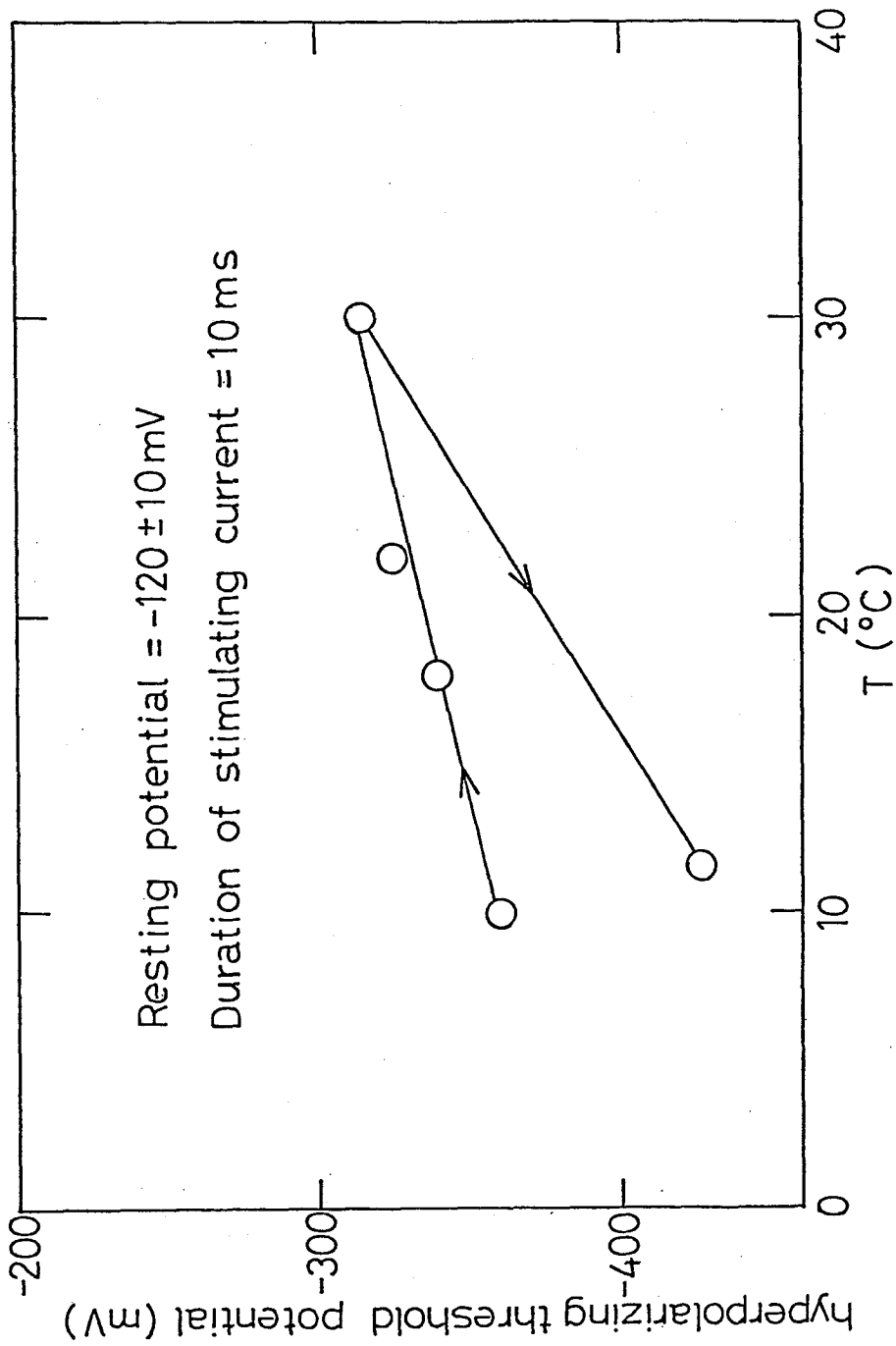


Fig. 18 Temperature dependence of hyperpolarizing threshold potential. Duration of the stimulus is 10 ms. Sample:810113.

IV. Model Calculations

A. Analysis of Delay

We examined to what extent the data presented in Fig. 10 can be explained based upon various trial models. Common assumptions in the analyses are as follows:

(a) The membrane current I_M is assumed to consist of the early transient current I_{Cl} , the potassium current I_K and the leakage current I_L : $I_M = I_{Cl} + I_K + I_L$.

In the previous study (Hirono and Mitsui 1981), we analyzed the membrane current during excitation according to the formulation by Beilby and Coster (1979 a,b,c). That is, we assumed that there is a common delay in the m and h gating and, after the delay, I_{Cl} and I_K are expressed by $I_{Cl} = \bar{g}_{Cl} m^3 h (V_M - V_{Cl})$ and $I_K = \bar{g}_K n^4 (V_M - V_K)$. The results of this previous study suggest that we may safely assume the following.

(b) We assume $m_0 = 0$ for the initial value of g_{Cl} when the holding potential is V_r . Walker and Hope (1969) demonstrated $g_{Cl} \ll g_K$ at V_r . Our previous study (Hirono and Mitsui 1981) indicated that the peak value of g_{Cl} is more than 20 times as large as g_K at the excitation. Therefore, it may be concluded that g_{Cl} at V_r is negligibly small compared to g_{Cl} at the excitation and thus m_0 may be approximated as zero.

(c) I_M , etc. just after the stepwise change of the membrane potential from V_r to V_M will be denoted as $I_M(0)$, etc. Then $I_{Cl}(0) = 0$ by the above approximation and thus $I_K(0) + I_L(0) = I_M(0)$. The current I_K increases very slowly, and the previous study

(Hirono and Mitsui 1981) suggests that we may put $I_K(t) + I_L(t) = I_M(0)$ for $t < 0.35$ s, $V_M = -40$ mV; $t < 0.45$ s, $V_M = -50$ mV; $t < 0.5$ s, $V_M = -60$ mV; $t < 0.59$ s, $V_M = -70$ mV; $t < 0.93$ s, $V_M = -90$ mV. Thus, in these time intervals, we assume

$$I_{Cl} = I_M - I_M(0) \quad (1)$$

Values of I_{Cl} calculated by Eq.(1) with I_M and $I_M(0)$ in Fig.10 will be given later by circles in Fig.20, 21 and 22.

(d) We assume that $h_\infty = 0$ in g_{Cl} for $V_M \geq -90$ mV since the previous study (Hirono and Mitsui 1981) showed $I_{Cl} \neq 0$ for $t > 4$ s, $V_M \geq -92$ mV.

On the assumptions (a)~(d), we examined validity of the following four models.

(i) $m^P h$ model

Keynes and Rojas (1976) reported that, in the squid giant axon, the $m^8 h$ model explained the initial part of the observed membrane current better than the $m^3 h$ model when the delay parameter δ was not introduced. We examined this type of model, treating the power of m as a variable together with other parameters. Now I_{Cl} is given by

$$I_{Cl} = \bar{g}_{Cl} m^P h (V_M - V_{Cl}). \quad (2)$$

The activation and inactivation parameters m and h were assumed to obey the same equations as Hodgkin and Huxley (1952 c) proposed:

$$\frac{dm}{dt} = \frac{1}{\tau_m} (m_\infty - m) \quad (3)$$

$$\frac{dh}{dt} = \frac{1}{\tau_h} (h_\infty - h) \quad (4)$$

According to the assumption (b) and (d), $m_0=0$ and $h_\infty=0$, and we have

$$m = m_\infty \{1 - \exp(-t/\tau_m)\} \quad (5)$$

$$h = h_0 \exp(-t/\tau_h). \quad (6)$$

Thus Eq.(2) becomes

$$I_{Cl} = \bar{g}_{Cl}' \{1 - \exp(-t/\tau_m)\}^p \exp(-t/\tau_h) (V_M - V_{Cl}), \quad (7)$$

where

$$\bar{g}_{Cl}' = \bar{g}_{Cl} m_\infty^p h_0. \quad (8)$$

We determined p , τ_m , τ_h and \bar{g}_{Cl}' so as to get the best agreement between calculated I_{Cl} and experimental I_{Cl} , which were derived by Eq.(1) with the data in Fig.10. The best agreement was not obtained with a constant p : $p=21$ for $V_M = -90$ and -70 mV; $p=15$ for -60 mV; $p=13$ for -50 mV; $p=15$ for -40 mV. Also we were forced to assign very large values to \bar{g}_{Cl}' . A relatively good agreement was obtained for the five values of V_M by fixing p as 18. Table 1 gives values of τ_m and τ_h and Fig.19 gives \bar{g}_{Cl}' in the case of $p=18$. We see \bar{g}_{Cl}' becomes anomalously large for low V_M in Fig.19.

According to Eq.(8), this fact implies that \bar{g}_{Cl}' increases anomalously at low V_M since m_∞ should decrease with decreasing V_M and h_0 is expected to be close to one. Therefore, the $m^p h$ model was discarded.

(ii) $m^p \{1 - (1-h)^q\}$ model

Table 1 τ_m and τ_h determined by curve fitting in $m^P h$ model

Parameter	V_M (mV)				
	-90	-70	-60	-50	-40
τ_m (s)	0.280	0.062	0.044	0.038	0.038
τ_h (s)	0.092	0.104	0.122	0.125	0.112

p=18. \bar{g}_{Cl} is shown in Fig. 19.

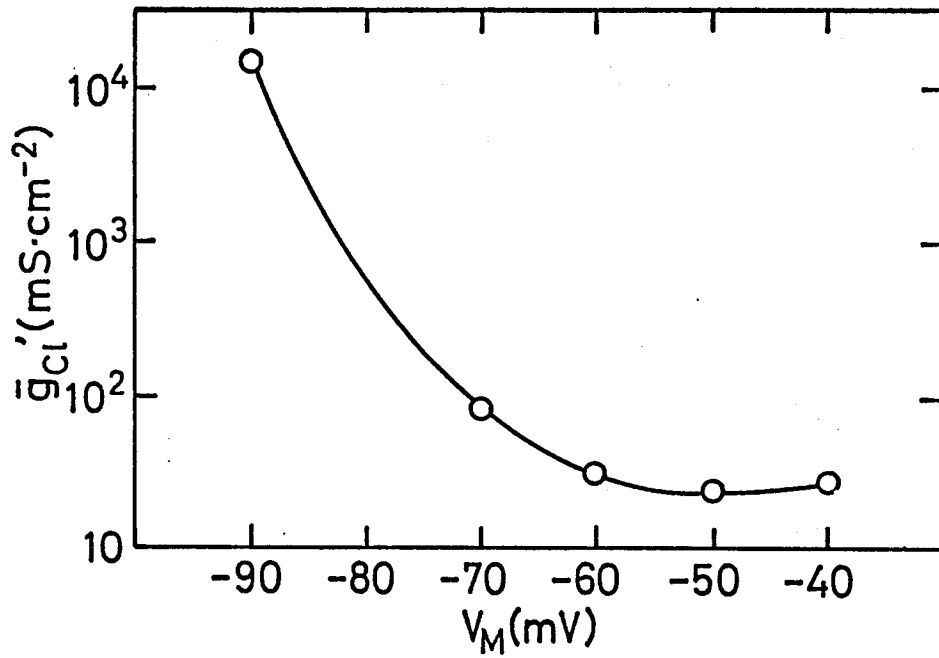


Fig. 19 \bar{g}_{Cl}' vs. V_M where $\bar{g}_{Cl}' = \bar{g}_{Cl} m_{\infty}^{18} h_0$. A result of $m^p h$ model when p was put equal to 18. Values of τ_m and τ_h used for the calculation are given in Table 1.

We examined this $m^p\{1-(1-h)^q\}$ model as an extension of the $m^p h$ model since we have $m^p h$ when we put $q=1$ in $m^p\{1-(1-h)^q\}$. A physical meaning of this model will be discussed in the Discussion. The expression of I_{C1} is

$$I_{C1} = \bar{g}_{C1} m^p \{1 - (1-h)^q\} (V_M - V_{C1}), \quad (9)$$

where

$$\left. \begin{aligned} m &= 1 - \exp(-t/\tau_m), \\ h &= \exp(-t/\tau_h). \end{aligned} \right\} \quad (10)$$

Here we put $m_0=0$, $h_\infty=0$ according to the assumption (b) and (d), and $m_\infty=1$, $h_0=1$ for simplicity since calculations suggested values of m_∞ and h_0 do not change the results seriously. Fig.20 shows I_{C1} derived by Eq.(1) with the data in Fig.10 by circles, which will be called observed I_{C1} below. We tested various values of \bar{g}_{C1} , p , q , τ_m and τ_h so as to get the best agreement between the observed and calculated I_{C1} . The solid lines in Fig.20 show calculated I_{C1} for the best agreement. In order to get good agreement, however, we were forced to assume that both p and q change to large extents depending upon V_M . Table 2 gives values of p , q , τ_m and τ_h . The values of p and q are indicated also in Fig.20. We see that very large values have to be assumed for p and q for low V_M , and thus this model was discarded.

(iii) $m^3 h - \delta$ model

This model was proposed by Beilby and Coster (1979 a,

Table 2 τ_m and τ_h used for calculation of I_{Cl} shown in Fig. 20

Parameter	V_M (mV)				
	-90	-70	-60	-50	-40
p	61	7	7	9	11
q	17	12	2	1	1
τ_m (s)	0.128	0.121	0.081	0.056	0.050
τ_h (s)	0.112	0.071	0.091	0.102	0.097

$\bar{g}_{Cl} = 46 \text{ mS} \cdot \text{cm}^{-2}$. $m^p \{1 - (1-h)^q\}$ model.

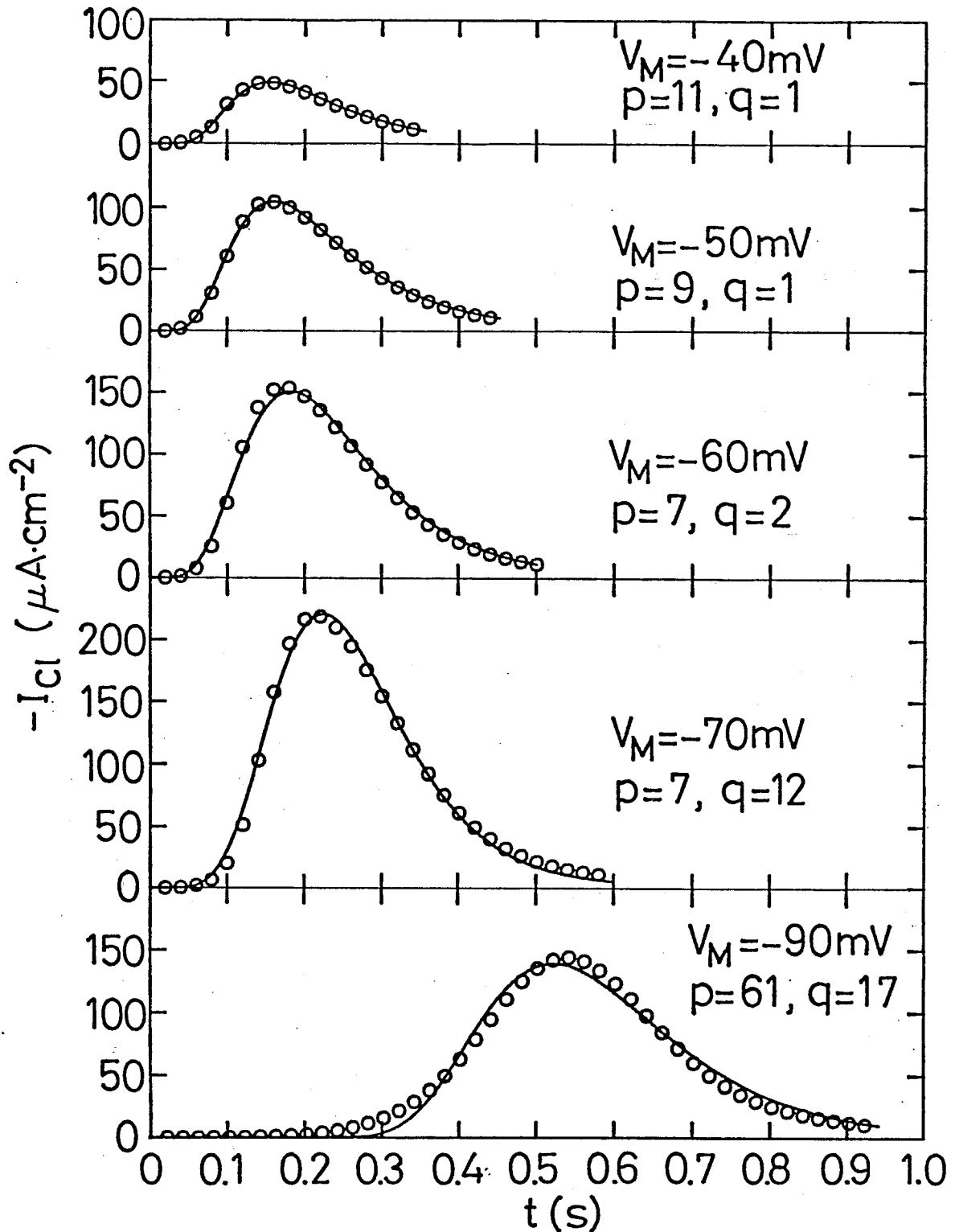


Fig. 20 Time courses of I_{Cl} at various clamp potentials V_M . $m^p\{1-(1-h)^q\}$ model. Circles: I_{Cl} obtained by Eq.(1) with I_M and $I_M(0)$ in Fig. 10. Solid lines: I_{Cl} calculated by Eqs.(9) and (10) with $\bar{g}_{Cl}=46 \text{ mS}\cdot\text{cm}^{-2}$ and $V_{Cl}=-31.5 \text{ mV}$. Values of p and q are indicated in each figure. Values of τ_m and τ_h used for the calculation are given in Table 2.

b, c) for *Chara corallina*. The expression for I_{Cl} is

$$I_{Cl} = \bar{g}_{Cl} m^3 h (V_M - V_{Cl}) \quad (11)$$

It was assumed that m and h do not change during the initial delay. We assumed that $m_\infty = 1$ and $h_0 = 1$ as in (ii), so that we have

$$m = 0 \text{ and } h = 1 \text{ for } 0 < t \leq \delta, \quad (12)$$

$$m = 1 - \exp\{(\delta - t)/\tau_m\}, \text{ for } t > \delta \quad (13)$$

and

$$h = \exp\{(\delta - t)/\tau_h\}, \text{ for } t > \delta. \quad (14)$$

where δ is a common delay time for the m and h gating. We determined \bar{g}_{Cl} , τ_m , τ_h and δ so as to get the best agreement between the observed and calculated I_{Cl} . Obtained results are given in Table 3. Value of \bar{g}_{Cl} was determined as $28 \text{ mS} \cdot \text{cm}^{-2}$. The values of all the parameters seem to be reasonable, but the observed I_{Cl} curves are not reproduced quite well as seen in Fig. 21. Especially discrepancy is evident in the rising phase of each curve, i. e., in the delay behaviour. As the delay behaviour was not explained well with the common delay δ , next we introduced two delay parameters δ_m and δ_h for the m and h gatings and examined the following model.

(iv) $m^p h - \delta_m - \delta_h$ model

The expression for I_{Cl} is given by

$$I_{Cl} = \bar{g}_{Cl} m^p h (V_M - V_{Cl}), \quad (15)$$

where

$$\left. \begin{aligned} m &= 0 \text{ for } 0 < t \leq \delta_m, \\ m &= 1 - \exp\{(\delta_m - t)/\tau_m\} \text{ for } t > \delta_m \end{aligned} \right\} \quad (16)$$

Table 3 Parameters used for calculation of I_{Cl} shown in Fig. 21

Parameter	V_M (mV)				
	-90	-70	-60	-50	-40
τ_m (s)	0.146	0.065	0.065	0.061	0.057
τ_h (s)	0.126	0.112	0.107	0.104	0.097
δ (s)	0.324	0.090	0.056	0.044	0.047

$\bar{g}_{Cl} = 28 \text{ mS} \cdot \text{cm}^{-2} \cdot \text{m}^3$ h- δ model.

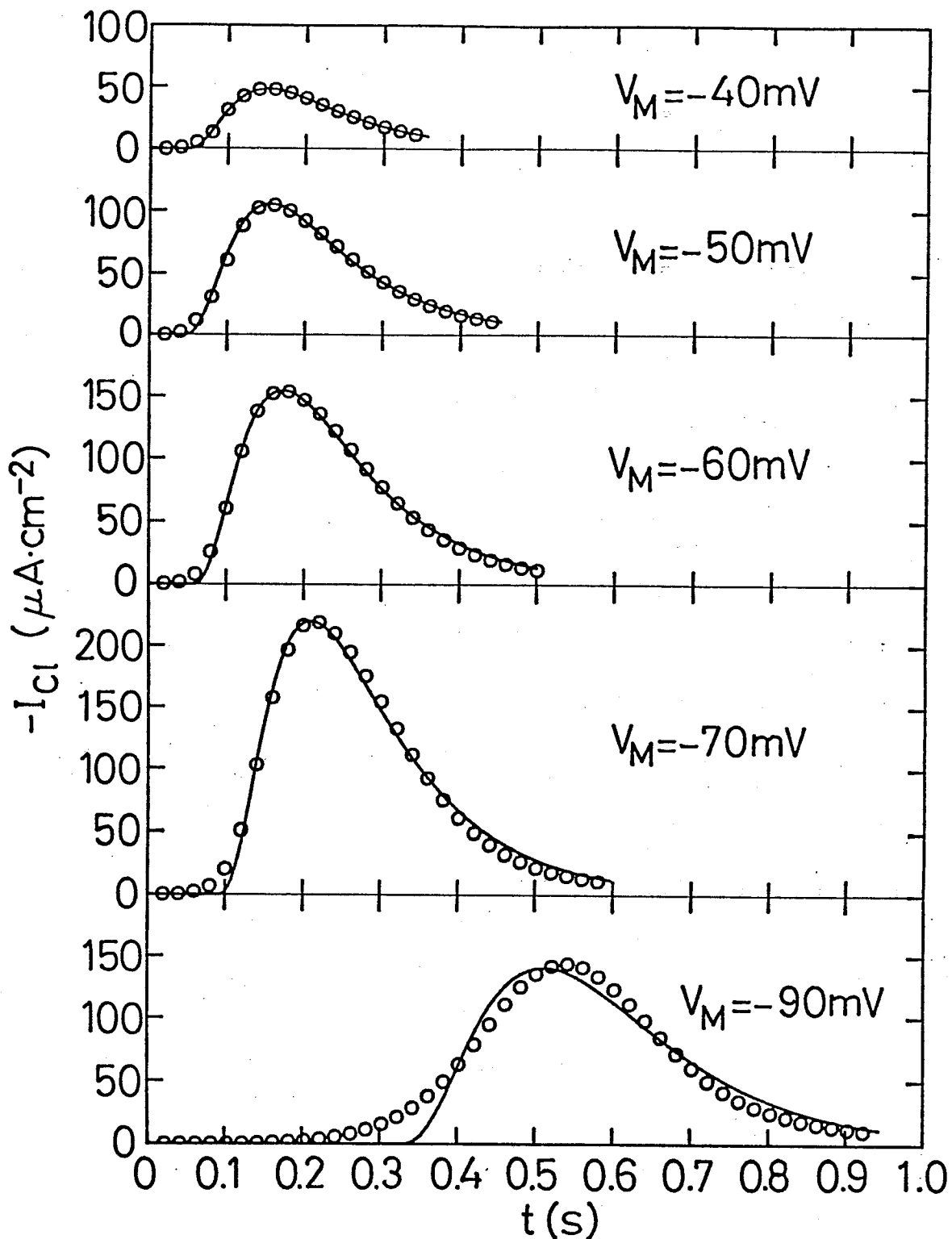


Fig. 21 Time courses of I_{Cl} at various clamp potential V_M . $m^3h-\delta$ model. Circles: the same as in Fig. 20. Solid lines: I_{Cl} calculated by Eqs.(11)~(14). Values of the parameters used for calculation are given in Table 3.

and

$$\left. \begin{aligned} h &= 1 \text{ for } 0 < t \leq \delta_h \\ h &= \exp\{(\delta_h - t)/\tau_h\} \text{ for } t > \delta_h \end{aligned} \right\} \quad (17)$$

We tried to get the best fit between the observed and calculated I_{Cl} by changing values of \bar{g}_{Cl} , p , δ_m , δ_h , τ_m and τ_h . Very good agreement was obtained as shown in Fig.22, with $\bar{g}_{Cl} = 15 \text{ mS}\cdot\text{cm}^{-2}$, $p=8$, $\delta_m=0$. Values of the other parameters are given in Table 4. The result of $\delta_m=0$ seems to be noteworthy and will be discussed in Discussion.

Table 4 Parameters used for calculation of I_{Cl} shown in Fig. 22

Parameter	V_M (mV)				
	-90	-70	-60	-50	-40
τ_m (s)	0.318	0.087	0.066	0.056	0.056
τ_h (s)	0.100	0.100	0.104	0.102	0.094
δ_h (s)	0.530	0.190	0.130	0.110	0.113

$p=8$, $\delta_m=0$, $\bar{g}_{Cl}=15 \text{ mS}\cdot\text{cm}^{-2}$. $m^p h-\delta_m-\delta_h$ model.

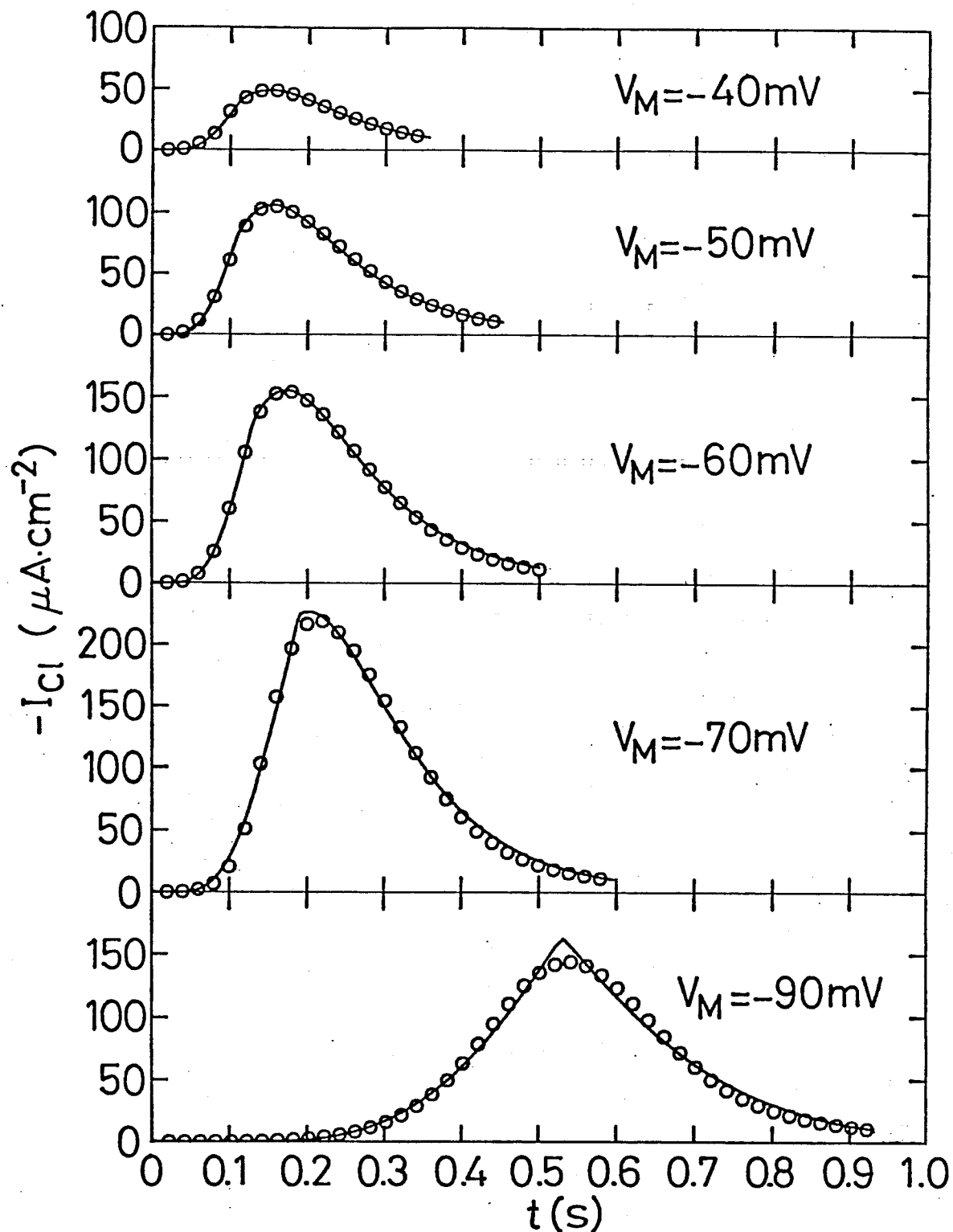


Fig. 22 Time courses of I_{Cl} at various clamp potential V_M . $m^P h - \delta_m - \delta_h$ model. Circles: the same as in Fig. 20. Solid lines: I_{Cl} calculated by Eqs. (15)~(17), with $p=8$ and $\delta_m=0$. Values of other parameters used for calculation are given in Table 4.

B. Reconstruction of Action Potential

Curve fitting of I_{Cl} by $m^8 h - \delta_h$ model resulted in good agreement between the calculation and observed data. In this section, $m^8 h - \delta_h$ model was examined by reconstruction of action potential. The reconstruction was made using two sets of data obtained from two specimens (i.e., sample Nos. 810515 and 781124). First the parameter set in Table 4 (sample No. 810515) was used to express τ_m and τ_h as function of V_M . τ_m is assumed to be expressed by:

$$\begin{aligned} \tau_m = & 1.1999 + 0.084075V_M + 0.0022922V_M^2 + 0.000027699V_M^3 \\ & + 0.00000012666V_M^4 \end{aligned} \quad (18)$$

where V_M is clamp potential (mV). τ_h can be approximated as 0.1 s at each V_M :

$$\tau_h = 0.1 \quad (19)$$

As for δ_h , it is not appropriate to express δ_h as a function of V_M when V_M changes. Fig. 23 shows the relationships between δ_h and V_M in two samples. Circles in Fig. 23 are the same data in Table 4. In these data δ_h is approximately two times as large as τ_m , that is, in voltage clamp $m = 1 - \exp(-2\tau_m/\tau_m) = 1 - \exp(-2)$ at $t = \delta_h = 2\tau_m$. So that it can be assumed that h begins to change when $m = 1 - \exp(-2)$.

In the model calculation, I_K was assumed to be very small and constant for $t < 0.35$ s, $V_M = -40$ mV; $t < 0.45$ s, $V_M = -50$ mV; $t < 0.5$ s, $V_M = -60$ mV; $t < 0.59$ s, $V_M = -70$ mV; $t < 0.93$ s, $V_M = -90$ mV. It is assumed that these limited domains in which $I_K + I_L$ is constant can be extended to the duration of reconstructed action potential.

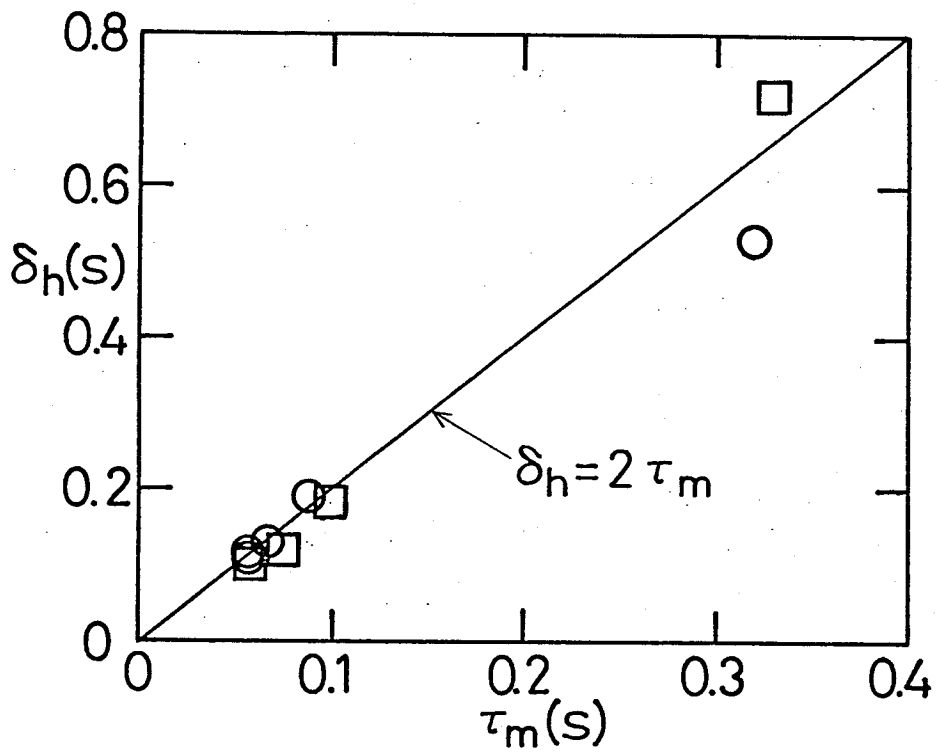


Fig. 23 Correlation between δ_h and τ_m determined curve fitting in $m^8 h - \delta_h$ model. Circles: sample 810515, squares: sample 781124.

Simultaneous derivative equations of V_M , m , h , n are expressed as follows:

$$\frac{dV_M}{dt} = \frac{1}{C_M} \{ I - \bar{g}_K n^4 (V_M - V_K) - \bar{g}_{Cl} m^8 h (V_M - V_{Cl}) \} \quad (20)$$

$$\frac{dn}{dt} = \frac{1}{\tau_n} (n_\infty - n) \quad (21)$$

$$\frac{dm}{dt} = \frac{1}{\tau_m} (m_\infty - m) \quad (22)$$

$$\frac{dh}{dt} = 0 \text{ for } \frac{dm}{dt} \geq 0 \text{ and } m \leq 1 - \exp(-2),$$

$$\frac{dh}{dt} = \frac{1}{\tau_h} (h_\infty - h) \text{ for } \frac{dm}{dt} < 0 \text{ or } m > 1 - \exp(-2) \quad (23)$$

where $C_M = 0.001 \text{ mF} \cdot \text{cm}^{-2}$, $\bar{g}_K n(0)^4 = 0.044 \text{ mS} \cdot \text{cm}^{-2}$, $\bar{g}_{Cl} = 15 \text{ mS} \cdot \text{cm}^{-2}$, $V_K = -140 \text{ mV}$, $V_{Cl} = -31.5 \text{ mV}$. $I_L = g_L (V_M - V_L)$ is neglected for simplicity. Boundary conditions are assumed as:

$$\begin{aligned} V_M(0) &= -140 \text{ mV} \\ \bar{g}_K n(0)^4 &= 0.044 \text{ mS} \cdot \text{cm}^{-2} \\ m(0) &= 0 \\ h(0) &= 1 \\ \bar{g}_K n_\infty^4 &= 0.044 \text{ mS} \cdot \text{cm}^{-2} \\ m_\infty &= 0 \text{ for } V_M \leq -95 \text{ mV} \\ m_\infty &= 1 \text{ for } V_M > -95 \text{ mV} \\ h_\infty &= 1 \text{ for } V_M < -139.99 \text{ mV} \\ h_\infty &= 0 \text{ for } V_M \geq -139.99 \text{ mV} \end{aligned} \quad (24)$$

Fig. 24 shows calculated action potential from Eqs. (20)~(24) by Runge-Kutta method with stimulation of 50 ms outward current. Amplitudes of the current is $3.5 \mu\text{A} \cdot \text{cm}^{-2}$ (a), $4.4 \mu\text{A} \cdot \text{cm}^{-2}$ (b) and $6.6 \mu\text{A} \cdot \text{cm}^{-2}$ (c).

Another reconstruction of action potential was made

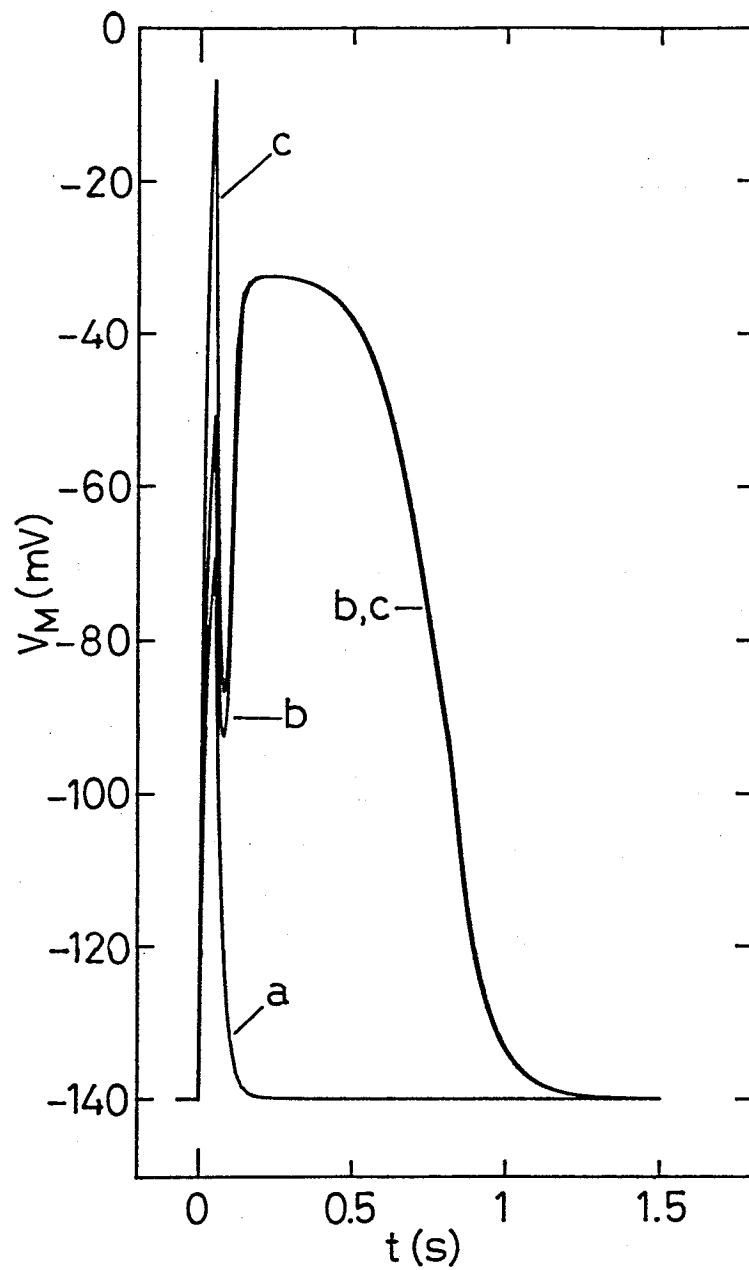


Fig. 24 Calculated action potential using the values of parameters given in Table 4. a: Subthreshold response to the current stimulation of $3.5 \mu\text{A}\cdot\text{cm}^{-2}$. b, c: Action potentials induced by the stimulation of $4.4 \mu\text{A}\cdot\text{cm}^{-2}$ (b), $6.6 \mu\text{A}\cdot\text{cm}^{-2}$ (c). Duration of the stimuli is 50 ms.

for the sample of which data were used in the analysis in 1979 (Hirono and Mitsui 1981). In this sample I_K is not negligible during excitation and voltage dependence of

n_∞ , m_∞ , h_∞ , τ_n , τ_m and τ_h are expressed by:

$$n_\infty = 1/[1 + \exp\{(-127 - V_M)/27.3\}]$$

$$m_\infty = 0 \text{ for } V_M \leq -94.99 \text{ mV}, m_\infty = 1 \text{ for } V_M > -94.99 \text{ mV}$$

$$h_\infty = 1 \text{ for } V_M \leq -119.99 \text{ mV}, h_\infty = 0 \text{ for } V_M > -119.99 \text{ mV}$$

$$\tau_n = 1 + 0.052 \exp(-V_M/14.43)$$

$$\tau_m = 0.42/[1 + \exp\{(V_M + 89.4)/3.71\}] + 0.05$$

$$\tau_h = 0.32/[1 + \exp\{(-82 - V_M)/11\}] + 0.1$$

The simultaneous derivative equations are the same as Eqs. (20) ~ (23), where $\bar{g}_K = 0.344 \text{ mS} \cdot \text{cm}^{-2}$, $\bar{g}_{Cl} = 2.9 \text{ mS} \cdot \text{cm}^{-2}$.

$V_K = -120 \text{ mV}$ and $V_{Cl} = -50.4 \text{ mV}$. Initial values are

$$V_M(0) = -120 \text{ mV}$$

$$n(0) = 0.564$$

$$m(0) = 0$$

$$h(0) = 1$$

Fig. 25A is reconstructed action potential with 50 ms outward current of which amplitude is $2 \mu\text{A} \cdot \text{cm}^{-2}$ (a), $2.25 \mu\text{A} \cdot \text{cm}^{-2}$ (b), $4.5 \mu\text{A} \cdot \text{cm}^{-2}$ (c). Observed action potential in the same sample, of which voltage clamp data was used to reconstruct the action potential in Fig. 25A, is shown in Fig. 25B. The peak height and the duration of calculated and observed action potentials are relatively in good agreement in this sample.

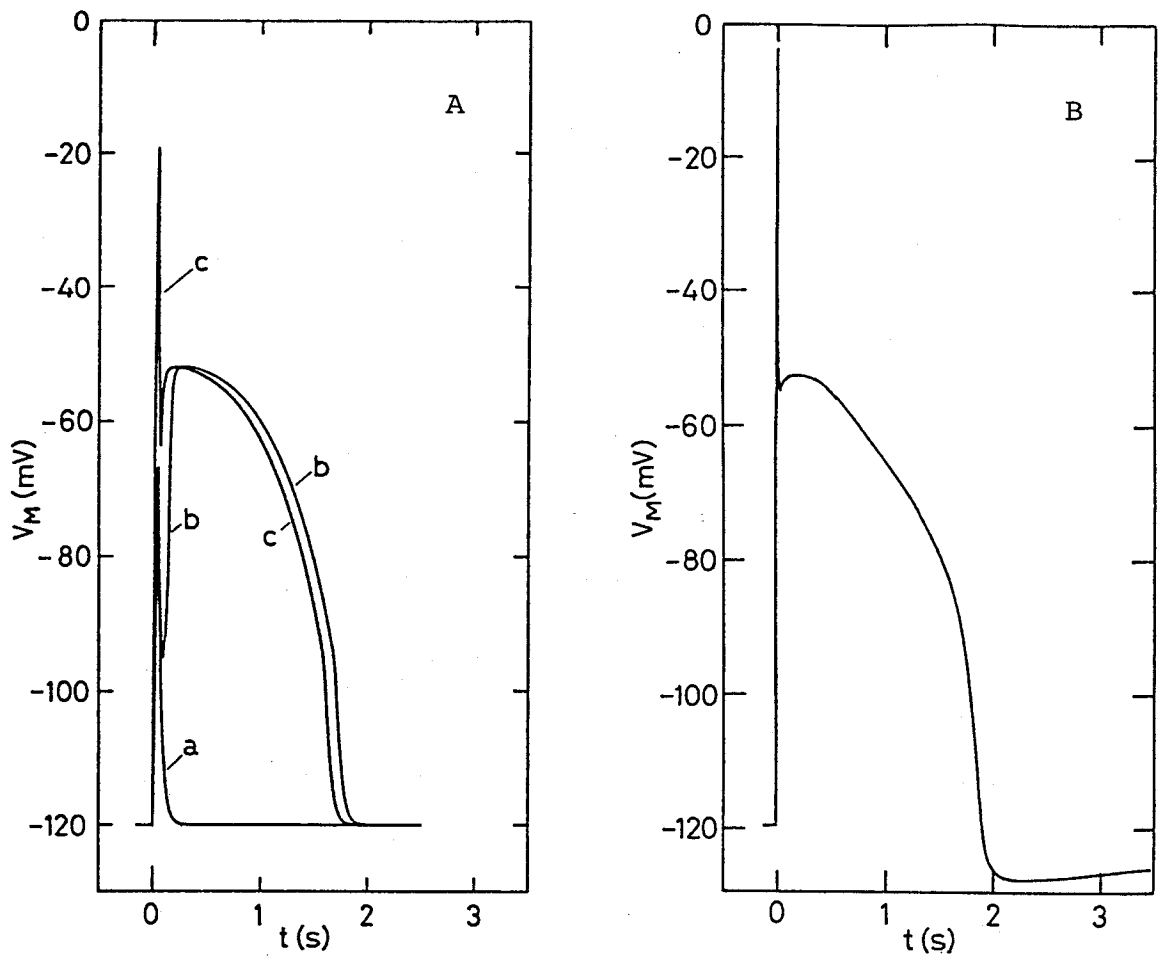


Fig. 25 Action potentials calculated from Eqs. (20)~(23) (A), with $\bar{g}_K=0.344 \text{ mS}\cdot\text{cm}^{-2}$, $\bar{g}_{Cl}=2.9 \text{ mS}\cdot\text{cm}^{-2}$, $V_K=-120 \text{ mV}$ and $V_{Cl}=-50.4 \text{ mV}$, and observed in Sample 781124 (B).

V. Discussion

As was described in the Introduction, the excitation in *Chara* and *Nitella* is associated with Cl^- efflux and K^+ efflux, and I_{Cl} in *Nitella* and *Chara* has the same function as I_{Na} in squid giant axon. In the present study, I_{Cl} is investigated. Separation of I_{Cl} from I_{M} should be made by changing the reversal potential of I_{Cl} , if possible, as was made by Hodgkin and Huxley for I_{Na} in squid giant axon (Hodgkin and Huxley 1952a). But it is difficult to change only the reversal potential V_{Cl} without changing $g_{\text{Cl}}(V,t)$ by increasing external Cl^- ion, because increase of Cl^- concentration induces irreversible change in $g_{\text{Cl}}(V,t)$ of plasmalemma. So that experimental separation of I_{Cl} from I_{K} and I_{L} was difficult by changing V_{Cl} . This difficulty was avoided by using the specimen in which I_{K} was very small compared to I_{Cl} as was mentioned in Experimental Results and will be discussed later.

Another point of difficulty in the analysis of the excitation is that *Nitella* and *Chara* have two membranes. Internodal cells of *Nitella* and *Chara* have large vacuoles which occupy more than 85% of the cell volume and cytoplasmic layers between plasmalemma and tonoplast are very thin ($\sim 10 \mu\text{m}$). A microelectrode for recording membrane potential is usually inserted into vacuole. It is not easy to analyse the excitation observed via plasmalemma and tonoplast, because membrane potential via plasmalemma

will change even if membrane potential via plasmalemma and tonoplast is clamped. Considering this point, Beilby and Coster (1979a, b, c) used young whorl cells of *Chara corallina*, which have larger space between plasmalemma and tonoplast than grown-up cells. They inserted a microelectrode for voltage recording, into cytoplasm between plasmalemma and tonoplast, and a wire electrode for current supply, into the central vacuole. On the other hand, we used single membrane samples from which major parts of vacuoles were removed by centrifugation and could easily insert a microelectrode into cytoplasm of the sample. As the sample was very short (≈ 1 mm in length) we inserted another microelectrode for intracellular current supply. It was experimentally proved that propagation does not affect the time course of excitation in the sample, that will be discussed later.

As mentioned in Experimental Results, some specimens gave very small I_K compared to I_{Cl} in a limited domain of membrane potential and others gave relatively large I_K . We used specimens of the former type and could study the properties of I_{Cl} separately. In the study we tacitly assumed that the variation in the ratio of I_K to I_{Cl} is caused by variation in density of channels from specimens to specimens. We examined three specimens in which I_K was very small. Obtained values of τ_m , τ_h and δ_h for one sample

were given in Table 4. Values of the parameters for the other two specimens were the same order of magnitude as those given in Table 4 except for \bar{g}_{Cl} . Values of \bar{g}_{Cl} which should depend upon the density of Cl channels were 15, 3 and 20 $\text{mS}\cdot\text{cm}^{-2}$ for three specimens. These results suggest that our assumption is close to reality.

The experimental results shown in Fig. 12 indicate that the delay is not caused by the low electric conductance of the external solution.

The data in Fig. 13 demonstrate that the delay is observed both in the light and dark and is not related to the light effect. Recently many workers reported the existence of electrogenic ion pump in *Chara* and *Nitella* as was described in Experimental Results. Voltage clamp data of membrane current which were measured in the light will contain the contribution of pump current, because the electrogenic pump is activated well in the light. Kishimoto et al. (1981) proposed a model of electrogenic H^+ pump in which pump conductance is voltage dependent but not time dependent. Following this model, pump current during voltage clamp will be constant and involved in I_L , so that it will be subtracted by Eq.(1).

The time course of I_{Cl} observed in the light is similar to that in the dark and delay behaviour did not seem to change by the light. The amplitude of I_{Cl} after setting the sample in the dark does not change or becomes smaller

than that in the light. This property of I_{Cl} was emphasized by decreasing the holding potential in the dark to the resting level in the light for 10 min. Therefore, the decrease of I_{Cl} may be caused by not only the change of resting potential but also other factor. The amplitude of I_{Cl} did not recover well after setting the sample in the light again.

The data given in Fig. 14 prove that the delay is not related to the propagation of change of the membrane potential. The propagation velocity of the action potential in an internodal cell of *Nitella flexilis* was reported as $200\sim 430 \text{ mm}\cdot\text{s}^{-1}$ in tap water (Sibaoka 1958). The specimen used to get the data in Fig.14 was cylindrical with the length of 1.7 mm and the diameter of 0.34 mm. Therefore, the propagation will be finished in about $(1.7/2) / 200 \text{ s} = 4 \text{ ms}$, which is negligibly small in the time scale in Fig.14 and thus the coincidence of the time courses of V_a and V_b is reasonable. From these observations we may conclude that the delay in current response to the stepwise change of V_M is inherent in the plasmalemma of *Nitella axilliformis*.

The existence of the delay required some modification in Hodgkin and Huxley's m^3h expression for the early transient current I_{Cl} of *Nitella* plasmalemma. We have examined the four modifications: (i) m^Ph , (ii) $m^P\{1-(1-h)^Q\}$,

(iii) $m^3h^{-\delta}$ and (iv) $m^p h^{-\delta_m - \delta_h}$ models. In the models (i) and (ii) we examined whether the observed behaviour of I_{Cl} could be explained without explicit introduction of delay parameters such as δ in (iii).

In the model (i), the expression $m^p h$ corresponds to assuming p pieces of m gates in series. Larger p values results in slower onset of I_{Cl} and thus an apparent delay. We were, however, forced to assume the sharp increase of \bar{g}_{Cl} at low V_M to explain the experimentally observed behaviours of I_{Cl} and discarded this model. Then we tried to introduce some modification in the h gating in a way similar to changing p in $m^p h$. Here it should be noted that h^q has mathematically the same meaning as changing τ_h as far as h is put proportional to $\exp(-t/\tau_h)$ and that effects of changing τ_h were already examined in the model (i). In terms of the channel model, $m^p h^q$ stands for a series connection of p pieces of m gates and q pieces of h gates. Fig.26A illustrates the case of $p=3$ and $q=2$, where each gate is depicted as a switch in a box and m and h mean the probabilities that the corresponding switches are on, i. e., the gates are open. If we change the connection of h gates from series connection (e. g., Fig.26A) to parallel connection (e. g., Fig.26B), the expression $m^p h^q$ turns into $m^p \{1-(1-h)^q\}$, i. e., the model (ii). If we put $h=\exp(-t/\tau_h)$ in $f(h)=1-(1-h)^q$, we have $f(h)=1-(t/\tau_h)^q$ for $t \ll \tau_h$. Thus $f(h; q \geq 2)$ causes slower decrease of I_{Cl} than $f(h; q=1)=h=\exp(-t/\tau_h)$,

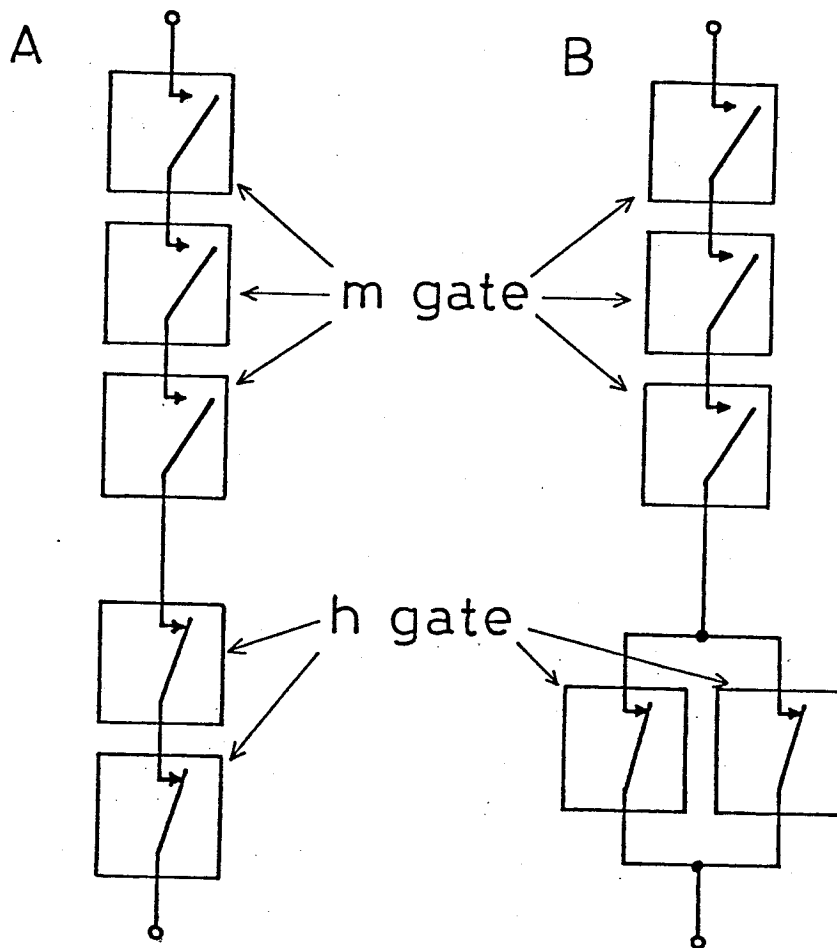


Fig. 26 A schematic representation of channel model.
 (A) $m^3 h^2$ model. (B) $m^3 \{1 - (1-h)^2\}$ model. Three m gates
 are in series and two h gates are parallel.

resulting in an apparent delay in inactivation. With this model, however, we could not keep both of p and q constant to explain the observed I_{Cl} .

In the model (iii), the common delay δ was assumed in the m and h gatings following Beilby and Coster (1979 a, b, c). We could not explain well the delay behaviours of I_{Cl} for *Nitella axilliformis* as seen in Fig.21. The delay parameter, however, does not seem to be necessarily common in the m and h gatings since they are different processes. In fact the time constant τ_m and τ_h depend upon V_M differently in Table 3. Therefore, we examined the model (iv), the $m^p h - \delta_m - \delta_h$ model. After many calculations with various trial parameters, we have found a very good agreement between the observed and calculated I_{Cl} as seen in Fig.22, with $p=8$, $\delta_m=0$ and the values of δ_h , τ_m , τ_h given in Table 4. The result $\delta_m=0$ means that we do not have to assume a delay mechanism in activation process of Cl channel if we put $p=8$. On the other hand, it is inevitable to assume the delay in inactivation process. Thus the delay observed in onset of I_{Cl} has the following two origins. Firstly eight m gates contribute to activation of the Cl channel so that the onset of I_{Cl} is slower than the $m^3 h$ case, resulting in an apparent delay. Secondly the h gating has an intrinsic delay δ_h . In Table 4, we see that δ_h and τ_m decrease with increasing V_M from -90 mV to -50 mV and then become rather steady. Since τ_m is approximately the time needed for the m gates

to open, this fact suggests that the h gates start to close after the m gates get open, resulting in delay δ_h in inactivation. One possible mechanism causing this delay might be as follows. In the resting state most m gates are closed and h gates open, so that the membrane potential drops effectively across the m gates, and much less across the h gates. The potential drop across the h gates will become appreciable when the m gates open associated with the stepwise change of V_M . Thus h gates start to close after the m gates open. Waiting for the increase of potential drop across the h gates will be observed as a delay in inactivation.

In the model (iv), the time course of I_{Cl} is expressed by Eqs. (15), (16) and (17). Therefore, there occurs a discontinuity in tangent of the calculated curve of I_{Cl} at $t=\delta_h$ as seen at $t=0.19$ s for $V_M=-70$ mV and at $t=0.53$ s for $V_M=-90$ mV in Fig. 22. These discontinuities were caused by the phenomenological introduction of constant δ_h by Eq. (17). It will be possible to remove these discontinuities by considering the mechanism causing δ_h such as described above.

Several authors reported a time lag in the inactivation process in excitable membranes. According to Armstrong (1970), inactivation of g_{Na} begins after a short time lag in *Dosidicus* axons. Goldman and Schauf (1972) observed a delay in inactivation of g_{Na} in *Myxicola* giant axons. In

giant axons from *Loligo pealei* and *Dosidicus gigas*, Bezanilla and Armstrong (1977) observed delayed onset of inactivation and proposed the model that the activation and inactivation processes are coupled in the Na channel and the inactivation does not occur until the channel opening is completed.

The value of V_{Cl} used in the calculations was -31.5 mV, which was determined by extrapolation of the maximum inward current vs. V_M curve, by using the data shown in Fig. 10. V_{Cl} thus determined for several samples were distributed in the range from about -50 mV to about -20 mV. The concentration of Cl^- was reported as 27 mM in protoplasm of *Nitella flexilis* (Tazawa et. al. 1974). The concentration of Cl^- in our APW was 0.25 mM. With these values, the Nernst potential of Cl^- across the plasmalemma is estimated as 118 mV, which is much larger than the above mentioned values of V_{Cl} , -50 mV \sim -20 mV. One possible explanation for this difference is that ions other than Cl^- also contribute to the transient current which we have denoted as I_{Cl} . The Nernst potentials estimated for Na^+ and K^+ are -50 mV and -185 mV respectively. Presumably K^+ can pass through the "Cl channel" and contribute to " I_{Cl} " and reduce the " V_{Cl} " from 118 mV to -50 mV \sim -20 mV.

Acknowledgements

The author would like to express sincere thanks to Prof. T. Mitsui (Faculty of Engineering Science, Osaka University) for his continuous advice, encouragement and valuable discussion throughout this study. He also thanks other members of this laboratory. He sincerely appreciates helpfull discussion and advice of Prof. U. Kishimoto (General Education, Osaka University), members of the laboratory and Prof. N. Iwasaki (Osaka Medical College). Thanks are due to Dr. K. Kuroda (Faculty of Science, Osaka University) who kindly supplied him with *Nitella axilliformis*, and Mr. K. Nakanishi in showing him a original FORTRAN program for calculation of action potential.

Reference

- Armstrong, C.M.: Comparison of g_K inactivation caused by quaternary ammonium ion with g_{Na} inactivation, *Biophys. Soc. Annu. Meet. Abstr.*, 10:185a, 1970.
- Beilby, M.J. and H.G.L. Coster: The action potential in *Chara corallina*; II. Two activation-inactivation transients in voltage clamps of the plasmalemma, *Aust. J. Plant Physiol.*, 6:323-335, 1979a.
- Beilby, M.J. and H.G.L. Coster: The action potential in *Chara corallina*; III. The Hodgkin-Huxley parameters for the plasmalemma, *Aust. J. Plant Physiol.*, 6:337-353, 1979b.
- Beilby, M.J. and H.G.L. Coster: The action potential in *Chara corallina*; IV. Activation enthalpies of the Hodgkin-Huxley gates, *Aust. J. Plant Physiol.*, 6: 355-365, 1979c.
- Bezanilla, F. and C.M. Armstrong: Inactivation of the sodium channel; I. Sodium current experiments, *J. Gen. Physiol.*, 70:549-566, 1977.
- Cole, K.S. and H.J. Curtis: Wheatstone bridge and electrolytic resistor for impedance measurements over a wide frequency range, *Rev. Sci. Inst.*, 8:333-339, 1937.
- Cole, K.S. and H.J. Curtis: Electric impedance of *Nitella* during activity, *J. Gen. Physiol.*, 22:37-64, 1938.
- Findlay, G.P. and A.B. Hope: Ionic relations of cells of *Chara australis*; VII. The separate electrical character-

- istics of the plasmalemma and tonoplast, *Aust. J. Biol. Sci.*, 17:62-77, 1964.
- Gaffey, C.T. and L.J. Mullins: Ion fluxes during the action potential in *Chara*, *J. Physiol.*, 144:505-524, 1958.
- Goldman, L. and C.L. Schauf: Inactivation of the sodium current in *Myxicola* giant axons; Evidence for coupling to the activation process, *J. Gen. Physiol.*, 59:659-675, 1972.
- Hayashi, T.: Some aspects of behavior of the protoplasmic streaming in plant cells, *Bot. Mag. Tokyo*, 65:51-55, 1952.
- Hirono, C. and T. Mitsui: Time course of activation in plasmalemma of *Nitella axilliformis*, in *Nerve Membrane - Biochemistry and Function of Channel Proteins*, Ed. by G. Matsumoto and M. Kotani, pp.135-149, University of Tokyo Press, Tokyo, 1981.
- Hodgkin, A.L. and A.F. Huxley: Action potentials recorded from inside a nerve fibre, *Nature*, 144:710-711, 1939.
- Hodgkin, A.L. and A.F. Huxley: Currents carried by sodium and potassium ions through the membrane of the giant axon of *Loligo*, *J. Physiol.*, 116:449-472, 1952a.
- Hodgkin, A.L. and A.F. Huxley: The dual effect of membrane potential on sodium conductance in the giant axon of *Loligo*, *J. Physiol.*, 116:497-506, 1952b.
- Hodgkin, A.L. and A.F. Huxley: A quantitative description of membrane current and its application to conduction and excitation in nerve, *J. Physiol.*, 117:500-544, 1952c.
- Kamiya, N. and K. Kuroda: Velocity distribution of the proto-

- plasmic streaming in *Nitella* cells, *Bot. Mag. Tokyo*, 69: 544-554, 1956.
- Keynes, R.D. and E. Rojas: The temporal and steady-state relationships between activation of the sodium conductance and movement of the gating particles in the squid giant axon, *J. Physiol.*, 255:157-189, 1976.
- Kishimoto, U.: Electrical characteristics of *Chara corallina*, *Ann. Rep. Sci. Works, Fac. Sci. Osaka Univ.*, 7:115-146, 1959.
- Kishimoto, U.: Electromotive force of *Nitella* membrane during excitation, *Plant & Cell Physiol.*, 9:539-551, 1968.
- Kishimoto, U., N. Kami-ike and Y. Takeuchi: The role of electrogenic pump in *Chara corallina*, *J. Membrane Biol.*, 55: 149-156, 1980.
- Kishimoto, U., N. Kami-ike and Y. Takeuchi: A quantitative expression of the electrogenic pump and its possible role in the excitation of *Chara corallina*, in *The Biophysical Approach to Excitable Systems*, Ed. by W.J. Adelman and D.E. Goldman, pp.165-181, Plenum Publishing Corporation, 1981.
- Kitasato, H.: The influence of H^+ on the membrane potential and ion fluxes of *Nitella*, *J. Gen. Physiol.*, 52:60-87, 1968.
- Marmont, G.: Studies on the axon membrane; I. A new method, *J. Cell. Comp. Physiol.*, 34:351-382, 1949.
- Nakanishi, K.: Hodgkin-Huxley's Equations and Excitation Due to Hyperpolarizing Stimulus (master's thesis, in Japanese), 1980.
- Ohkawa, T. and U. Kishimoto: Anode break excitation in *Chara*

- membrane, *Plant & Cell Physiol.*, 16:83-91, 1975.
- Richards, J.L. and A.B. Hope: The role of protons in determining membrane electrical characteristics in *Chara corallina*, *J. Membrane Biol.*, 16:121-144, 1974.
- Saito, K. and M. Senda: The electrogenic ion pump revealed by the external pH effect on the membrane potential of *Nitella*; Influences of external ions and electric current on the pH effect, *Plant & Cell Physiol.*, 15:1007-1016, 1974.
- Shimmen, T. and M. Tazawa: Control of membrane potential and excitability of *Chara* cells with ATP and Mg^{2+} , *J. Membrane Biol.*, 37:167-192, 1977.
- Sibaoka, T.: Conduction of action potential in the plant cell, *Trans. Bose. Res. Inst.*, 22:43-56, 1958.
- Tazawa, M., U. Kishimoto and M. Kikuyama: Potassium, sodium and chloride in the protoplasm of Characeae, *Plant & Cell Physiol.*, 15:103-110, 1974.
- Walker, N.A.: Microelectrode experiments on *Nitella*, *Aust. J. Biol. Sci.*, 8:476-489, 1955.
- Walker, N.A. and A.B. Hope: Membrane fluxes and electric conductance in Characean cells, *Aust. J. Biol. Sci.*, 22: 1179-1195, 1969.

Appendix

Electric Circuit for Measurements

Analog Circuit

Operational amplifiers were used to compose the analog circuit for measuring and controlling the membrane potential and / or the membrane current of the sample. Fig.A-1 shows the diagram of the circuit which was used in most of this study. It consists of eight operational amplifiers: Amp.1 and Amp.2, model 1026 (Teledyne Philbrick); Amp. 3 and Amp.5, model LF356 (National Semiconductor); Amp.4, model 40J (Analog Devices); Amp.6, model 1032 (Teledyne Philbrick). The voltage of power supply are ± 15 V for Amp.1 ~ Amp.5 and ± 110 V for Amp.6. The circuit for measuring membrane potential which consists of Amp.1~3, is high input impedance, differential amplifier. Voltage gain of the circuit is 10. Amp.4 and 5 compose a current-voltage converter. Output voltage of the the converter is given by: $V=2 \times 10^6 \cdot I$. With Amp.1~3, Amp.6 composes negative feedback loop as to the membrane potential via plasmalemma (i.e., glass microelectrode for voltage record \rightarrow Amp.1 \rightarrow Amp.3 \rightarrow Amp.6 \rightarrow glass microelectrode for current supply \rightarrow membrane potential). As the glass microelectrode is of high resistance, Amp.6 needs to have high gain and high voltage output enough to charging the membrane capacitance instantaneously.

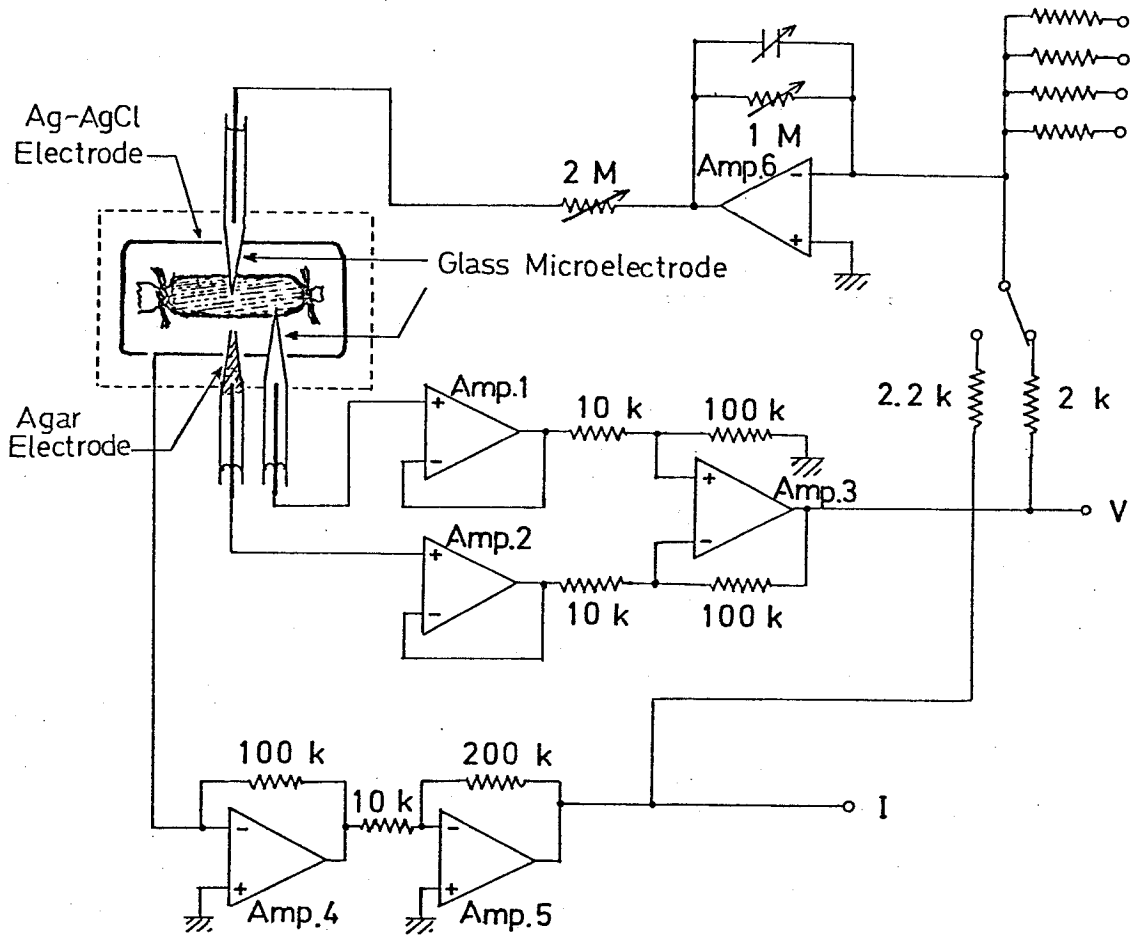


Fig. A-1 Diagram of the circuit for the measurement of membrane potential and the membrane current, for stimulation by pulsed current and for voltage clamp.

Digital Circuit

The block diagram of data entry system in the present study are illustrated in Fig. A-2. The data of V_M and I_M measured with the analog circuit shown in Fig. A-1 are selected, converted to digital data with A/D converter AD80AG-12 (Micro Network Corp.) and stored into semiconductor memory by micro-computer (Lkit-16). After a measurement, the digital data are converted to analog data with D/A converter DAC-HZ12BGC (Datel Systems, Inc.) and drawn on the chart of X-Y recorder. The speed ratio of reconstructing the data to sampling the original data can be changed from $1 \sim 1/2560$. The digital data used for analyses is recorded on the magnetic tape with digital cassette MT-2 (TEAC). The data can be transmitted from MT-2 to micro-computer MINC-11 (DEC) or mini-computer PDP 11/34 (DEC) via micro-computer H68/TR (Hitachi) and GPIB interface with MC68488 (Motorola).

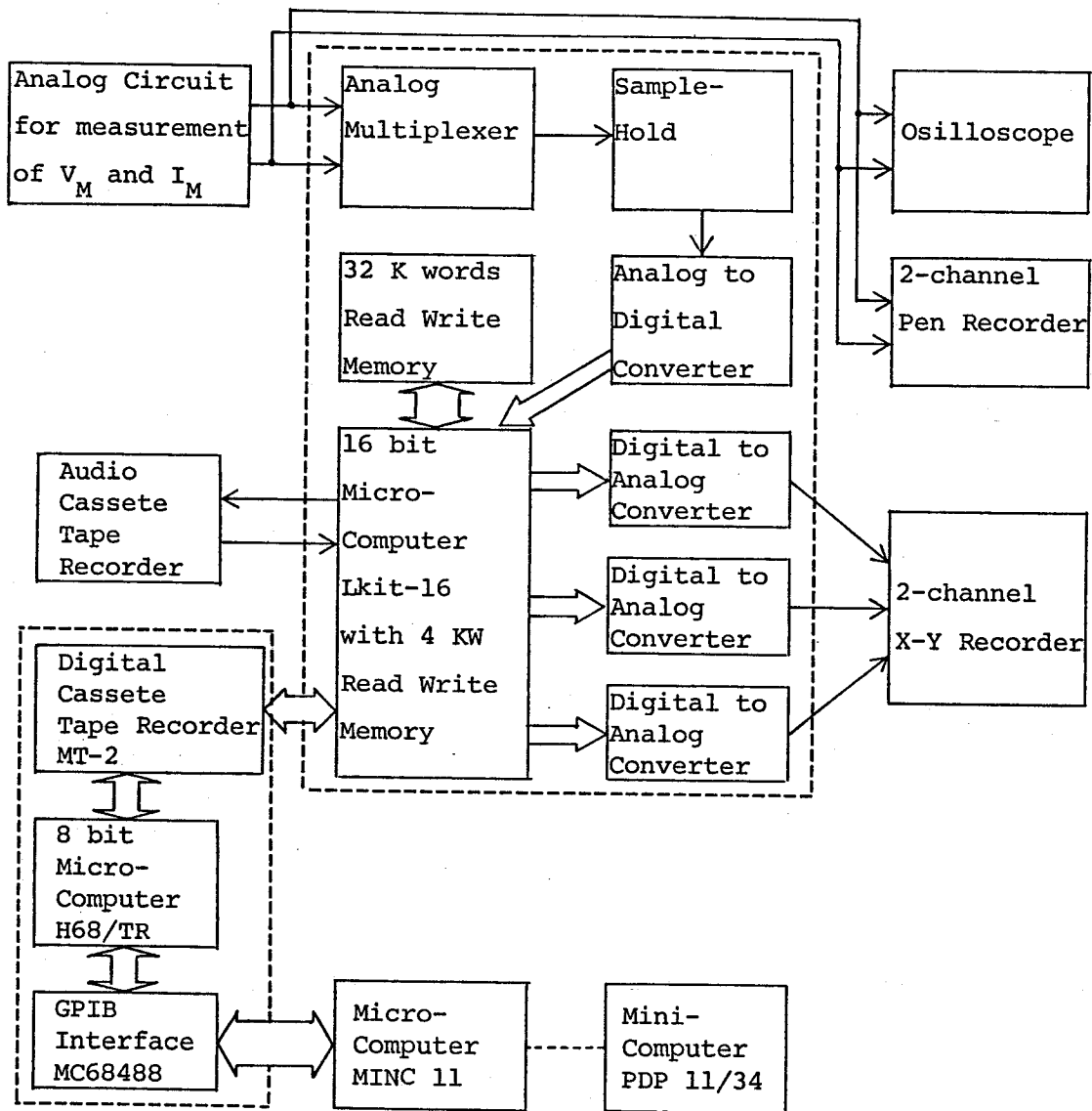


Fig. A-2 Block diagram of data entry system which consists of two parts included by broken lines. Main part is a large scale memory with analog-to-digital and digital-to-analog converters which are controlled by a 16 bit CPU MN1610 (Panafacom). The other is a digital cassette tape recorder which can be controlled by the main part or by a GPIB controller (e. g., MINC 11).